University of Stavanger

Faculty of Science and Technology

MASTER'S THESIS

Study program/ Specialization: Industrial Economics / Petroleum Technology	Spring semester, 2014 Open / Restricted access
Writer: Nina Frøyland	…… (Writer's signature)
Faculty supervisor: Olav Gerhard Haukenes Nygaard External supervisor(s):	
Thesis title: Automatic evaluation and adjustment of drilling fluid properties and compositions during MPD operations and its cost-benefit analysis	
Credits (ECTS):	
Key words: Fann® 35 Viscometer Dual DP Drilling Fluid Evaluation Differential Pressure Pressure Loss Calculations	Pages: 55 + enclosure: 10 Stavanger, 13.06.2014 Date/year

Abstract

During drilling operations it is important to keep the pressure in the well intact. The drilling fluid provides pressure, but its purpose is also to keep the formation fluids in place and at the same time lubricate the drill bit. For the fluid to perform well, there are especially five properties that needs monitoring; density, rheology, fluid loss, solids content and chemical properties.

Today the evaluation of the drilling is in a large extent performed manually on a laboratory at the drilling facility. The workers go through special courses and training programs to be able to execute the tests, they are also exposed to chemical hazards and the stress of being responsible for drilling operation stops.

The new way of thinking is to automate the whole drilling fluid evaluation system, for a safer and more reliable process. The idea is to implement a system that will test the properties of the mud, and then adjust it accordingly.

By changing the drilling fluid evaluation process from manually to automatically the system will be more cost efficient as the error margin is smaller, the system gives an improved drilling performance and reduced environmental impact.

In this thesis the differential pressure system Dual DP, originated at the University of Stavanger, is employed to test differential pressure of a fluid flow. From this, several properties of the fluid can be calculated including the density and viscosity. In addition, the Fann® 35 rheometer's diversity gets a review, to see if there are ways to get more accurate results. Several spring sensitivities are applied.

Acknowledgements

This thesis is part of the study concerning automation of the evaluation and adjustment of the most important properties of the drilling fluid. It is a joint project made possible by the University of Stavanger, Statoil, IRIS and NTNU. This is my contribution as a Master of Science student within Industrial Economics with Petroleum Technology as specialization.

I would like to take this opportunity to thank my supervisor *Professor Olav Gerhard Haukenes Nygaard*, for being such a great mentor by giving me good feedback and further guidance. I very much appreciate the chance I got to participate in this exciting project. I would also like to thank *Tor Henry Omland* at Statoil for his involvement relative to the thesis.

I would like to thank the employees responsible for purchasing chemicals and other lab necessities for providing rapid service, and a special thanks to *Sivert Bakken Drangeid* for helping me prepare both of the laboratories and being a part of the process from the beginning.

I would like to thank fellow students at the University of Stavanger for their help, support and companionship. And a special thanks to *Ida Halvorsen Verpe*, for taking the time to help me understand the basics of the flow loop system in these busy times.

A special thanks to *Anne Sissel Svendsen* , student counselor at the Industrial Economics department, for facilitating the whole Master of Science program to my benefit. I appreciate it.

I would like to thank my family; mother *Vibeke*, father *Bjarne*, brother *Marius* and sister *Charlotte* for supporting me and for believing in me through my studies. An extra thanks to my sister for taking the time to review my thesis.

Last but not least, I would like to thank *Vegard Dyrseth*, for being supportive and making the whole process a little bit easier.

Nomenclature

Symbol	Description	Unit
$\boldsymbol{A}$	Viscometer constant	$\frac{cP \times rpm}{deg}$
$\boldsymbol{A_1}$	Flow area	m^2
$\boldsymbol{A_g}$	Bob-rotor geometry constant	$\frac{cP \times rpm}{dyne - cm}$
$\boldsymbol{B}$	Viscometer constant	$\frac{cP \times rpm}{lb\ per\ 100\ sq\ ft}$
$\boldsymbol{D}$	Diameter of the pipe	m
$\boldsymbol{dP_{hor}}$	Hortizontal differential pressure	Pa
$\boldsymbol{dP_{ver}}$	Vertical differential pressure	Pa
$\frac{\boldsymbol{dv}}{\boldsymbol{dr}}$	Velocity gradient	$\frac{1}{s}$
$\boldsymbol{F}$	Force of fluid flow	$\frac{kgm}{s^2}$
$\boldsymbol{f_{lam}}$	Friction factor – laminar flow	
$\boldsymbol{f_{turb}}$	Friction factor – turbulent flow	
$\boldsymbol{g}$	Gravitational acceleration	$\frac{kgm}{s^2}$
$\boldsymbol{K}$	Consistency index	$\frac{dynes}{cm^2}$
$\boldsymbol{K_s\ and\ k_1}$	Spring constant	$\frac{dyne - cm}{deg}$
$\boldsymbol{k_2}$	Shear stress constant for effective bob surface	$sec^{-1}\ per\ rpm$
$\boldsymbol{k_3}$	Shear rate constant	$\frac{1}{cm^3}$
$\boldsymbol{L}$	Length of the pipe	m
$\boldsymbol{L_b}$	Length of bob/annulus	$dyne - cm$
$\boldsymbol{L_e}$	Correction factor	$dyne - cm$
$\boldsymbol{n}$	Flow behavior index	
$\boldsymbol{P}$	Pressure	Pa
$\boldsymbol{P_0}$	Initial pressure needed for movement	Pa
$\boldsymbol{P_h}$	Hydrostatic pressure	Pa
$\boldsymbol{P_d}$	Dynamic fluid pressure loss	Pa
$\boldsymbol{P_p}$	Pump pressure	Pa

Symbol	Description	Unit
$\boldsymbol{PV}$	Plastic viscosity	cP
$\boldsymbol{Q}$	Volumetric flow rate	$m^3 s$
$\boldsymbol{r}$	Radius of the pipe	m
$\boldsymbol{R_b}$	Radius of the bob	cm
$\boldsymbol{R_c}$	Radius of the cylinder	cm
$\boldsymbol{Re}$	Reynolds number	
$\boldsymbol{T}$	Torque	$dyne - cm$
$\boldsymbol{T_0}$	Torque at yield point	$dyne - cm$
$\boldsymbol{T_1}$	Critical torque	$dyne - cm$
$\boldsymbol{T_2}$	Torque intercept	$dyne - cm$
$\boldsymbol{V}$	Average velocity	$\frac{m}{s}$
$\boldsymbol{YP}$	Yield point	$\frac{lb}{ft^2}$
$\boldsymbol{\tau}$	Shear stress	$\frac{lb}{ft^2}$
$\boldsymbol{\tau_0}$	Initial shear stress	$\frac{lb}{ft^2}$
$\boldsymbol{\gamma}$	Shear rate	$\frac{1}{s}$
$\boldsymbol{\mu}$	Viscosity	cP
$\boldsymbol{\mu_e}$	Effective viscosity	cP
$\boldsymbol{\mu_p}$	Plastic viscosity	cP
$\boldsymbol{\omega}$	Rotor speed	rpm
$\boldsymbol{\bar{\omega}}$	Angular velocity	$\frac{rad}{s}$
$\boldsymbol{\omega_L}$	Laminar flow of the annulus	$\frac{rad}{s}$
$\boldsymbol{\theta}$	Dial reading	$^\circ\, dial\ reading$
$\boldsymbol{\rho_l}$	Density of the fluid	$\frac{kg}{m^3}$
$\boldsymbol{\rho_o}$	Density of silicone oil	$\frac{kg}{m^3}$
$\boldsymbol{\nu}$	Kinematic velocity	$\frac{m^2}{s}$
$\boldsymbol{\epsilon}$	Roughness for drawn tubing	m

List of figures

List of tables

List of plots

List of equations

Table of contents

Chapter 1 INTRODUCTION

During drilling operations the borehole needs drilling fluid, more commonly called “mud”, to keep the pressure of the well stable. The mud will also lubricate the drill bit and bring the cuttings out of the way and up to the surface. All this needs to be done without damaging the borehole, as well as the environment above and around the drilling facility. To keep control of the stability of the well there are five basic properties that need constant monitoring during the drilling operation; density, rheology, fluid loss, solids content and chemical properties [1]. In this thesis, only density and rheology are taken into consideration.

Today the drilling fluid evaluation procedure is generally conducted manually by mud engineers. These engineers need proper training and courses to execute this type of work. The time spent on manual work may cause operational stops, and the consequences of entering the wrong results in the mud report, can be great [2]. Also, as the petroleum industry is redirecting the work to new areas with more unstable formations, the need for a continuous update on the drilling fluids properties is highly necessary. An automated system will provide a more reliable monitoring system which will result in better well control during drilling operations [3]. The main driving force for implementing this automated system is that it provides a cost effective drilling operation, as well as the employee safety against exposure is improved and the system is more reliable in general. [1; 2].

When the drilling fluid is tested, the rig crew calculates the necessity of the different components and adjusts the fluid accordingly, to maintain the stability of the fluid. There are new ways to automate this process, and previous students of the University of Stavanger have been working on a new flow loop that can be used for such purposes. The Dual DP is a flow system with dual differential pressure sensors on a horizontal and a vertical profile. The system is built to measure the differential pressure from one sensor to the next along the profile. From these measurements, the apparent viscosity and density can be calculated [4].

The Fann® 35 is the most common viscometer used in the oil industry for measuring the rheology of a drilling fluid [5]. This type of viscometer is used both in the research process as well as during production due to the wide range of application; the viscometer gives rheology values for both Newtonian and non-Newtonian fluids. The standard Fann® 35 viscometer is equipped with an R1 rotor sleeve, a B1 bob and an F1 torsion spring, but there are several combinations of these three available for further testing [6]. The drilling fluid probably represents around 5% to 15% of the total costs of drilling a well, meaning it is a big part of the drilling costs. An automated system might lower the costs by providing a more accurate and an enhanced drilling performance [1].

1.1 Motivation and problem description

The drilling industry faces new challenges as the years go by and more and more of the oil in place is extracted from the reservoirs. Further, this means that the search field is expanding to new areas and the drilling operations may become more complex. When drilling through a more complex formation, the drilling fluid needs to fulfill certain demands to make sure the borehole stays intact. The evaluation of drilling fluids will be harder, and the margin of error becomes smaller. The need for an automated drilling fluid system is growing as the complexity of the fluids grows and continuous monitoring is essential to keep the fluids characteristics in order.

The University of Stavanger has together with Statoil, IRIS and NTNU, started to look at a new method of automatically testing the properties of drilling fluids in motion. The method consists of a flow loop with four pressure sensors connected giving the horizontal and the vertical differential pressure. The "Dual DP" system was built by former students at the university, which makes the project very interesting. The system has only been tested with water so far, and the most desirable thing to do next is to test how the system behaves when a fluid with different characteristics than water is applied.

Today, the drilling fluid evaluation is mostly performed manually with the Fann® 35 rheometer. When using the Fann® 35 viscometer to measure the rheology of a fluid, there is an uncertainty in the readings of the lower speeds. The misreading of the Fann® 35 dial may lead to misinformation which can affect what engineers choose to do next. The thesis tries to shine a light on these misreadings, and looking at ways to improve them. Hopefully, the results collected here may contribute to the Dual DP project in some way in a later study.

1.2 Objective and scope

The main objectives of this thesis are;

- Perform a literature survey on drilling fluid evaluation
- Look at the functionality of the viscometer Fann® 35 with three different springs
- Get to know the Dual DP system and its functional application area and further give an explanation of how to operate the system
- Shortly elaborate on the economic consequences of changing to an automated drilling mud system

The literature study of this thesis has mostly been provided by the thesis supervisor, but also from the university library and several verified sources online.

The University of Stavanger provided two labs for the practical part of the thesis; the drilling fluids lab and the fluid flow lab. The mixing and testing regarding the Fann® 35 is executed in the drilling fluids lab and the Dual DP tests in the fluid flow lab.

Three Fann® 35 rheometers were delivered from Phoenix Trading AS. The rheometers were delivered with a certain modification; the rheometers were equipped with three different springs together with an associated calibration fluid for two of them.

The Dual DP system and its coherent theory was presented through the previous work of Kurt Louis Krogsæter, an MSc student graduated 2013 from the University of Stavanger.

Chapter 2 RHEOLOGY THEORY

The drilling fluid systems are many and complex, and one important aspect of evaluating the drilling fluids properties is to look at the viscosity. This is very important because it is vital for the well development that the drilling fluid remains intact during operations to prevent cave-ins, collapses etc. The viscosity is evaluated by measuring its rheology; the study of the flow of matter. The rheology has developed greatly within the liquid phase flow. There are two main relationships; the laminar flow regime (low flow velocities) and the turbulent flow regime (high flow velocities). A laminar flow regime has an orderly flow, which means that it is possible to look at the relationship between pressure and velocity as a function of the viscous properties of a fluid. With a turbulent flow regime the flow is disorderly and therefore the equations become empirical as the inertial properties of the flow are used [7].

2.1 Types of flow

There are four important flow models when looking at drilling fluid theory; the *Newtonian*, the *Bingham plastic*, the *pseudoplastic* and the *dilatant.* The curves of these flow models are illustrated in Figure 1. The dilatant is of little importance to this thesis, as no shear thickening fluid is used in drilling fluid technology. The three other models are fundamentally important within drilling fluid theory. They give the equations of the behavior relative to the characteristics of the drilling fluid itself. Most of the drilling fluids fall into a mix of these flow models, making it difficult to decide only one. The flow models give an impression of the behavior of the drilling mud, which is sufficient when evaluating it practically and further get a simulation coherent enough. The flow models are shown as curves, where shear stress is plotted against shear rate, or the flow pressure is plotted against the flow rate [7].

The different types of flows reveal different trends on the consistency diagram; the Newtonian has a straight line from origin, while the two other flow models are curved; pseudoplastic is shear thinning and dilatant is shear thickening, see Figure 1 below.

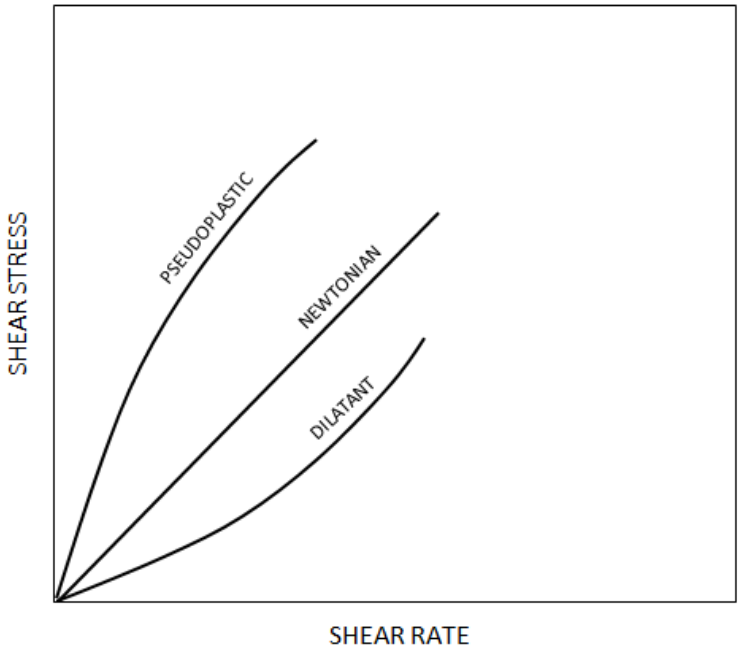

Figure 1 – Consistency curves showing three types of fluid flows

2.2 Newtonian fluids

The force of a fluid flow F divided by the flow area A_1 gives the shear stress, and it is further expressed with the shear rate $\frac{dv}{dr}$ and the frictional resistance to movement in the fluid itself viscosity μ in Equation 2-1.

$$\frac{F}{A_1} = \tau = -\mu \frac{dv}{dr} \qquad \textit{Equation 2-1}$$

The Newtonian fluid consistency curve is, as mentioned above, a straight line through the origin. The slope of the line is defined as the fluid's viscosity;

$$\mu = \frac{\tau}{\gamma} \qquad \textit{Equation 2-2}$$

where shear stress τ is divided by shear rate γ. The special thing with the Newtonian fluid is that having only one parameter, the viscosity μ, is sufficient to characterize the flow behavior of the fluid, as shown in Figure 2.

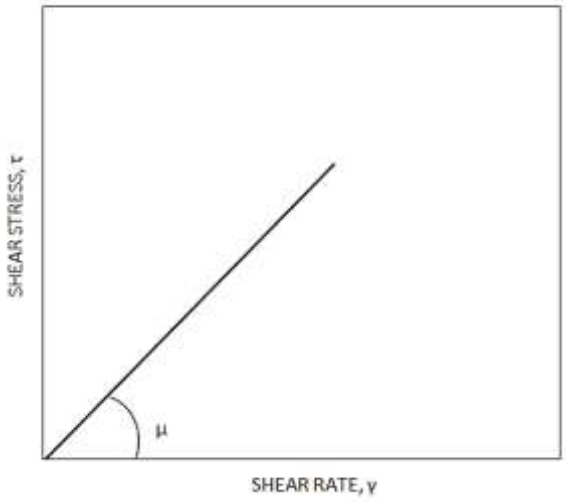

Figure 2 – Consistency curve of a Newtonian fluid

A Newtonian fluid passing through a pipe will automatically create a parabolic velocity profile as seen in Figure 3. The velocity profile takes this form because of the tension from the wall of the pipe. The shear rate dv/dr varies along the parabolic feature, and it is represented by the slope at that specific point of interest along the profile, as illustrated in Figure 3.

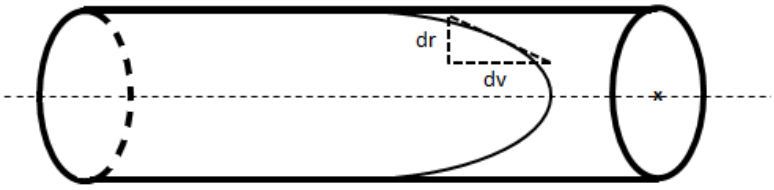

Figure 3 – Velocity profile in a pipe

The maximum shear rate is along the wall, where dr = 0. In the center of the pipe the shear rate is zero, as the slope of the parabolic feature is only represented by the dr.

When looking at the overall pressure versus the flow rate in this pipe, a shear stress equation is generated;

$$\tau = \frac{F}{A_1} = \frac{\pi r^2 \mathrm{P}}{2\pi r L} = \frac{rP}{2L} \qquad \textit{Equation 2-3}$$

where F is the force exerted by the fluid, A_1 is the cross sectional area of the pipe, P is the pressure, L the length and r is the radius of the pipe. When substituting for the shear stress τ as expressed in Equation 2-1, a new relationship is made;

$$\frac{rP}{2L} = -\mu \frac{dv}{dr} \qquad \textit{Equation 2-4}$$

This relationship further leads to the following equation;

$$Q = \frac{g\pi r^4 P}{8L\mu} \qquad \textit{Equation 2-5}$$

where Q is volumetric flow rate and r is the radius of the pipe. Equation 2-5 is also known as Poiseulle's laminar flow equation, for Newtonian fluids flowing through a pipe. See Gray and Darley, p. 185, for further information [7].

2.3 Bingham Plastic

The Bingham plastic flow model was chosen as the best alternative for describing drilling fluid behavior already in the early thirties. After analyzing the drilling fluid based on this law of flow, it was recognized as the best way to describe the laminar flow for most of the oil based drilling fluids [8].

The basic difference between a Bingham plastic fluid compared to the Newtonian, is that the Bingham plastic fluid needs a certain amount of initial stress to start flowing, while Newtonian flows right away. For an ideal Bingham plastic fluid the consistency curve will start at the initial shear stress τ_0 and then it will act like a Newtonian fluid, see Figure 4Figure 4. The equation of the Bingham plastic fluid is as followed;

$$\tau - \tau_0 = -\mu_p \frac{dv}{dr} \qquad \textit{Equation 2-6}$$

where μ_p is the plastic viscosity. When solving for shear stress, the equation for the consistency curve is defined;

$$\tau = \tau_0 + \mu_p \gamma \qquad \textit{Equation 2-7}$$

The difference between Newtonian and plastic flow becomes even clearer as the equation for plastic viscosity is defined;

$$\mu_p = \frac{\tau - \tau_0}{\gamma} \qquad \textit{Equation 2-8}$$

where γ is the shear rate. To explain the total resistance of the plastic fluid the effective viscosity is a necessity. The effective viscosity consists of two parts; the plastic viscosity as defined above, and; structural viscosity, which is the resistance to movement due to the buildup of structures between the particles in the fluid. The structural viscosity is the part of the process where the shear stress is increasing but the fluid is not moving until a certain stress τ_0 is reached, as illustrated in Figure 4.

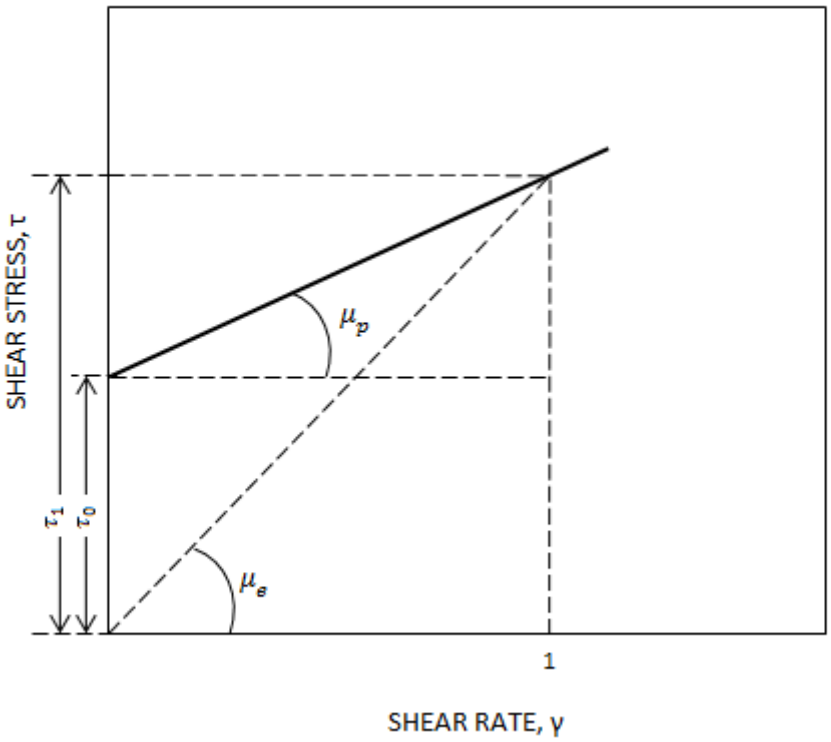

Figure 4 – Effective viscosity of a Bingham plastic fluid

The plastic viscosity together with the structural viscosity leads to the equation;

$$\mu_e = \frac{\tau - \tau_0}{\gamma} + \frac{\tau_0}{\gamma} = \mu_p + \frac{\tau_0}{\gamma} \qquad \textit{Equation 2-9}$$

where μ_e is the effective viscosity at a given shear rate γ. Effective viscosity will not be helpful unless the shear rate is known, both parameters are necessary for defining the viscous properties of a fluid.

For plastic flow in a pipe, the trend is to obtain the structural viscosity at first, followed by the movement of the fluid, now with a plastic viscosity. When gradually applying more pressure; it will take the form of a plug flow with radius R surrounded by a laminar flow with a varying velocity profile. In other words, the plug flow is a 'cylinder' in the middle of the pipe, between this cylinder and the pipe wall there is a section of laminar flow.

Equation 2-3 expresses the shear stress in a pipe; and in this case the initial shear stress needed for the first movement is;

$$\tau_0 = \frac{rP_0}{2L} \qquad \textit{Equation 2-10}$$

where P_0 is the initial pressure sufficient for movement, and r is the radius of the pipe. When applying even more pressure to the flow some of the plug flow will go over to the laminar flow phase, but there will always be a column of plug flow in the center. This is because P will increase when R decreases, and to get R = 0, P will have to become infinitely large. The consistency curve of a Bingham plastic will always be non-linear in a pipe system, but there are ways of approximating this curve. This is done by looking at the values along the curve when the flow rate is much higher. By making a straight line through these values back to the flow pressure axis, the line will cross the axis at 4/3 of P_0. An equation has been derived where the interception at 4/3 of P_0 and the Poiseulle's equation was combined;

$$Q = \frac{\pi r^4}{8\mu_p L}\left(P - \frac{4}{3}P_0\left(1 - \frac{P_0^3}{4P^3}\right)\right) \qquad \textit{Equation 2-11}$$

Substituting for $P_0=2L\tau_0/r$:

$$V = \frac{PD^2}{32\mu_p L}\left(1 - \frac{4}{3}\left(\frac{4\tau_0 L}{DP}\right) + \frac{1}{3}\left(\frac{4\tau_0 L}{DP}\right)^4\right) \qquad \textit{Equation 2-12}$$

Where V is the average velocity and D is the diameter of the pipe. The last part of Equation 2-12; $\frac{1}{3}\left(\frac{4\tau_0 L}{DP}\right)^4$, represents the area between the extended line and the curve. When looking at very high rates, this part can be excluded, as the significance will be too low. At very low rates the plug flow needs to be included in the equation. Plug flow is defined by;

$$V = \frac{\pi DkP}{2\mu L} \qquad \textit{Equation 2-13}$$

where k is a constant. For more information see Gray and Darley 1980, p 188-189 [7].

2.3.1 The coaxial cylinder rotational viscometer

The best way to determine plastic viscosity and the yield point is to use a coaxial cylinder rotation viscometer. The basic viscometer has an outer cup that rotates and inside an inner bob hangs in a wire, and the annulus between them is approximately 1 mm. When the cup is rotating, the bob experiences a drag around its own axis. This drag will continue until the resistance in the fluid is as big as the torque of the wire. When the bob has stopped, the rheology value can easily be read off at a dial. At this point the following equation applies;

$$\tau_0 = \frac{T_0}{2\pi R_b^2 L_b} \qquad \textit{Equation 2-14}$$

where T_0 is the torque at yield point, R_b is the radius of the bob and L_b is the height of the bob. Further in the rotation process there will be a laminar flow in the annulus, starting from the bob going outwards. When all the fluid in the gap is in laminar flow the equation changes;

$$\tau_0 = \frac{T_1}{2\pi R_c^2 L_b} \qquad \textit{Equation 2-15}$$

where T_1 is the critical torque and R_c is the radius inside the cup. When increasing the speed of the cup constantly, the torque will set on an equilibrium value, dependent on the rheological values of the fluid. The torque and speed will then have a proportional relationship creating a linear laminar flow of the annulus at ω_L, as shown in Figure 5. This is defined by the Reiner-Riwlin equation:

$$\bar{\omega} = \frac{T}{4\pi L_b \mu_p}\left(\frac{1}{R_b^2} - \frac{1}{R_c^2}\right) - \frac{\tau_0}{\mu_p} ln \frac{R_c}{R_b} \qquad \textit{Equation 2-16}$$

where $\bar{\omega}$ is the angular velocity in radians per second and T is the corresponding torque.

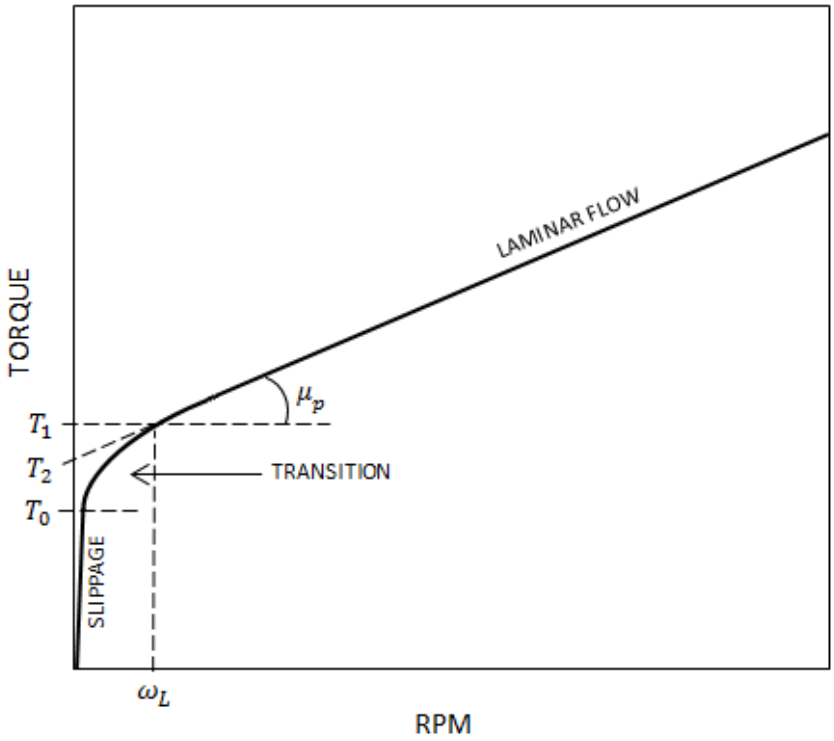

Figure 5 – The consistency curve of a Bingham plastic flow

2.3.2 The Couette type viscometer – a direct indicating viscometer

The rotational viscometer used in this study is a direct-indicating viscometer designed by Savins and Roper [8]. This viscometer is based on their theory that the Reiner-Riwlin equation can be simplified to;

$$\mu_p = \frac{A\theta - B\tau_0}{\omega} \qquad \textit{Equation 2-17}$$

where ω is the rotor speed in rpm and θ is the dial reading. A and B are constants that include the necessary conversions factors, instrument dimensions, and the spring constant. Further the plastic viscosity is defined by;

$$\mu_p = \overline{PV} = A\left(\frac{\theta_1 - \theta_2}{\omega_1 - \omega_2}\right) \qquad \textit{Equation 2-18}$$

where θ_1 and θ_2 is the dial reading registered at the velocities ω_1 and ω_2 and $\overline{PV}$ is the plastic viscosity. For the yield point $\overline{YP}$;

$$\tau_0 = \overline{YP} = \frac{A}{B}\left[\ \theta_1 - \left(\frac{\omega_1}{\omega_1 - \omega_2}\right)(\theta_1 - \theta_2)\ \right] \qquad \textit{Equation 2-19}$$

Now, the constants A and B, together with the velocities ω_1 and ω_2 were carefully selected so that;

$$A = B = \omega_1 - \omega_2$$

and the relationship between the two velocities are;

$$\omega_1 = 2\omega_2$$

under the given conditions that

$$\frac{A}{\omega_1 - \omega_2} = 1\,, \qquad \frac{A}{B} = 1, \qquad \frac{\omega_1}{\omega_1 - \omega_2} = 2$$

This further leads to that the equations; Equation 2-18 and Equation 2-19, becomes less complicated;

$$\overline{PV} = \theta_1 - \theta_2 \qquad \textit{Equation 2-20}$$

$$\overline{YP} = \theta_2 - \overline{PV} \qquad \textit{Equation 2-21}$$

To make this work the values of R_b and R_c were selected so that the value of $A = B$ was 300 when the annulus width was 1 millimeter. Accordingly, the rotor speed ω_2 had to be 300 and ω_1= 600 rpm. To make it possible to keep A = 300, the spring constant had to be 387 dyne centimeters per degree. Due to these specifications the PV is now in centipoise and the YP in pounds per 100 square feet. The readings from the direct-indicating viscometer can be used to find both the effective and apparent viscosity.

1° dial reading = 1.067 $\frac{lb}{100ft^2}$ = 5.11 $\frac{dynes}{cm^2}$ *Shear stress*

1 rpm = 1.703 reciprocal seconds *Shear rate*

$\mu_e = \frac{5.11}{1.703}$ poise per degree per rpm = 300 cP per degree per rpm = $\frac{300\times\theta}{\omega}$ *Effective viscosity*

$\overline{AV} = \frac{300 \times \theta_{600}}{600} = \frac{\theta_{600}}{2}$ *Apparent viscosity*

The apparent viscosity is used as an alternative to the effective viscosity.

2.3.3 Viscosity at low shear rates

As mentioned earlier, Bingham plastic fluids will have a linear curve after laminar flow is developed in the annulus, which matches drilling fluids behavior perfectly at high rates. But at low rates the drilling fluids deviate from this theory when using a direct-indicating viscometer. The flow in the annulus is fully laminar when

$$\frac{T}{2\pi R_c^2 L_b} > \overline{YP} \qquad \textbf{Equation 2-22}$$

When substituting for YP in the Equation 2-16;

$$\bar{\omega}_L = \frac{\overline{YP}}{2\overline{PV}}\left(\frac{R_c^2}{R_b^2} - 1 - 2ln\frac{R_c}{R_b}\right) \qquad \textbf{Equation 2-23}$$

And by using the instrumental constant the equation is

$$\omega_L = 20.62\frac{\overline{YP}}{\overline{PV}} \qquad \textbf{Equation 2-24}$$

where ω_L is the lowest possible rpm for laminar flow. Viscosity also differs with the quantity, size and shape of particles in a drilling mud. In addition, the electrochemical environment will determine the interparticle forces. But these factors are only mentioned to give a better impression of the things that can influence the drilling fluids behavior. As the drilling fluids properties vary the consistency curve changes. Looking at only the YP and PV is not always sufficient to predict the degree of deviation from linearity and the way of the curve itself, this is better done with a viscometer. Although, it might be used in a drilling mud evaluation at the well site, as an indication of what treatment is needed to better the fluid's performance. The PV and YP can also help predict the laminar flow in pipes, by applying these values to Equation 2-12, but only for high rates. For more information see Gray and Darley p. 194 [7]. For low rates the effective viscosity is better determined by the power law.

2.4 Power law

The power law is an empirical equation defined by;

$$\tau = K\left(\frac{dv}{dr}\right)^n = K\gamma^n \qquad \textit{Equation 2-25}$$

where K is the consistency index and n is the type of fluid, or the 'flow behavior index'. The consistency index corresponds to the viscosity of a Newtonian fluid, but it is expressed in dynes/cm^2. Equation 2-25 gives the consistency curve of a *pseudoplastic* fluid. The typical pseudoplastic fluid has no yield point, meaning the curves intercept at the origin. But at high rates the stress readings can be noted and extrapolated back to the axis, giving a "yield point" which gives a resemblance to the Bingham plastic. The constant K gives the viscosity of a Newtonian fluid as mentioned, and the n contains the degree of deviation from Newtonian behavior. If n is below 1, the fluid is a pseudoplastic fluid. When rearranging Equation 2-25, a logarithmic relationship appears;

$$\log\tau = \log K + n(\log\gamma) \qquad \textit{Equation 2-26}$$

which can be applied to a logarithmic plot giving a straight line as a function of the shear stress versus shear rate. The n will then represent the slope of the line and K is where the line intercepts the shear stress.

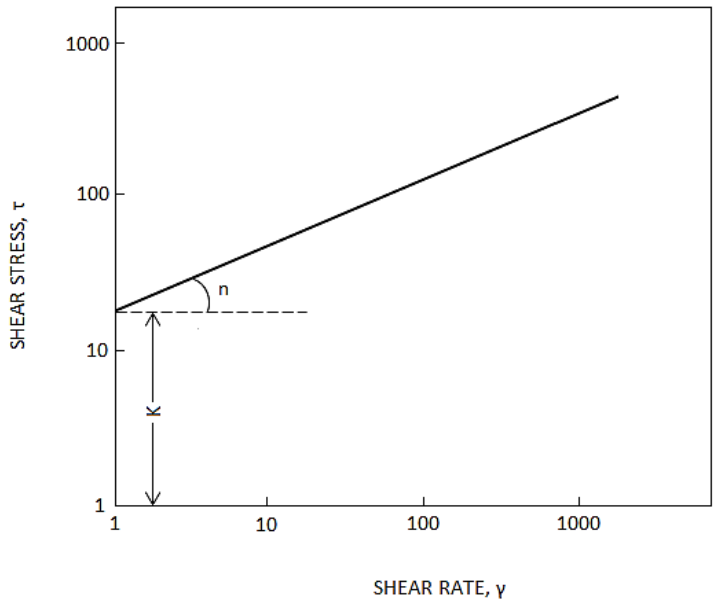

Figure 6 – Logarithmic plot of an ideal power law consistency curve

It is possible to find the n by using values from two known points along the line;

$$n = \frac{\log \tau_1 - \log \tau_2}{\log \gamma_1 - \log \gamma_2} \qquad \textit{Equation 2-27}$$

To find K either one of the equations below are applicable;

$$\log K = \log \tau_1 - \log \gamma_1 \qquad \textit{Equation 2-28}$$

$$K = \frac{\tau_1}{\gamma_1^n} \qquad \textit{Equation 2-29}$$

And further the effective viscosity of the pseudoplastic fluid is defined by;

$$\mu_e = \frac{\tau}{\gamma} = \frac{K\gamma^n}{\gamma} = K\gamma^{n-1} \qquad \textit{Equation 2-30}$$

2.5 Herschel-Bulkley

Most of the drilling fluids used today do not fall into only one of the flow models above. They are a mix of the ideal Bingham plastic and the ideal power law. This modified power law is constructed to cover the more diverse fluids. These fluids do not have a linear logarithmic line, nor constant n and K values, which makes it difficult to explain their flow behavior with only the Bingham plastic or the power law [7]. The Herschel-Bulkley flow model is a combination of these two flow models, and it is also known as the yield power law [9]:

$$\tau = \tau_0 + K\gamma^n \qquad \textit{Equation 2-31}$$

This model applies more to the flow in pipes than the flow in a Couette-type viscometer, where the Bingham plastic is better. The Herschel-Bulkley describes measured data best.

2.6 Influence of temperature and pressure on the rheology

The rheological properties of the drilling fluid may change due to temperature and pressure differences in the well. Both the temperature and the pressure will change along the path of the drilling mud. The physically, chemically and electrochemically properties of the fluid, are the properties who are most commonly influenced by these parameter changes. The changes of the parameters will bring changes to the characteristics of the fluid; the viscosity depends on both temperature and pressure, it decreases when the temperature increases. An increase in pressure will generate a higher viscosity due to a denser fluid. When mud reaches certain temperatures the chemical characteristics of the fluid will change. One possible reaction is that hydroxides will react with clay minerals, which usually happens when the mud reaches a temperature above 94°C. The electrochemical changes are based on how good the ionic connections between the particles are; with higher temperatures the ionic activity increases making the particles attract or repulse each other, which will influence how the rheological features are.

2.7 Pressure calculations for Dual DP plots

The pressure loss calculations will briefly be mentioned in this thesis, with focusing only on the equations needed to get the desired plots. For more information concerning this theory see Krogsæter's Master Thesis, 2013 [10].

The Dual DP system is a flow loop with four pressure sensors installed. The pressure sensors gather information which can be used to make several plots through MATLAB®. The following calculations are based on the assumption that the fluid is a Newtonian fluid. The pump pressure P_p is defined by;

$$P_p = \rho_l g L \qquad \textit{Equation 2-32}$$

where ρ_l is the density of the fluid, g is the gravitational acceleration constant and L is the length of the pipe.

In addition, the pump pressure is a sum of two pressure components; the dynamic fluid pressure loss P_d and the hydrostatic pressure P_h;

$$P_p = P_d + P_h \qquad \textit{Equation 2-33}$$

where the dynamic fluid pressure loss is further defined by;

$$P_d = dP_{ver} - dP_{hor} \qquad \textit{Equation 2-34}$$

and the hydrostatic pressure is defined by;

$$P_h = \rho_o g L \qquad \textit{Equation 2-35}$$

The dP_{ver} is the vertical differential pressure, dP_{hor} is the horizontal differential pressure and ρ_o is the density of the silicone oil found in the pressure sensors. As mentioned earlier in section 2.2 the fluid velocity is;

$$V = \frac{Q}{A} \qquad \textit{Equation 2-36}$$

which is a less complicated version of Equation 2-5, with main focus on the velocity. Further there are several equations to calculate the remaining properties:

The Reynolds number:

$$Re = \frac{VD}{\nu} = \frac{\rho_l VD}{\mu} \qquad \textit{Equation 2-37}$$

where ν is the kinematic viscosity, which is the viscosity of a fluid divided by its density, as seen in Equation 2-37. V is still the fluid velocity and D is the diameter of the pipe. The Reynolds number is a dimensionless quantity, and this quantity gives the ratio of the inertial forces to viscous forces.

The friction factor for laminar flow:

$$f_{lam} = \frac{64}{Re}$$ ***Equation 2-38***

which is the Darcy/Moody friction factor and is applicable for Re < 2300, above this the flow is turbulent and the friction factor is then

$$\frac{1}{\sqrt{f_{turb}}} = -1.8\log_{10}\left[\left(\frac{\frac{\epsilon}{D}}{3.7}\right)^{1.11} + \frac{6.9}{Re}\right]$$ ***Equation 2-39***

And friction loss through the pipe:

$$P_d = \frac{fL\rho_l V^2}{2D}$$ ***Equation 2-40***

Chapter 3 METHODOLOGY

The practical part of the thesis was divided into two groups; Fann® 35 and Dual DP, both with assignments in form of lab work. The Fann® 35 lab assignment involved both mixing and testing of certain fluids. These fluids were KCl brines with different amounts of DUO-TEC NS added to the brine. The M-I SWACO product DUO-TEC NS is a viscosifier of xanthan gum. This viscosifier gives the fluid shear thinning characteristics [11], meaning the fluids mixed at the lab are non-Newtonian. The brine was mixed in two separate volumes; one with a specific gravity, or 'SG', of 1.05 and another with 1.15. These brines were then split in three parts and different amounts of DUO-TEC NS were added, giving a total of six mixes, see Table 1.

MIX NO.	SG KCl BRINE	DUOTEC NS (g/l)
1	1,05	1
2		2
3		4
4	1,15	1
5		2
6		4

Table 1 – Overview of the six mixes

The components of the mixes were carefully chosen for such reason that they can easily be disposed down the drain after the testing on the Dual DP system is performed. Although the Dual DP testing in this thesis was solely with water, the mixes were made as plausible fluids for next year's Dual DP lab.

3.0.1 Fluid calibration Check

The three different Fann® 35 rheometers were checked before use, to see if the calibrations were correct. They were performed after point 6.2 in the instructions in the "Model 35 Viscometer – Instruction Manual" by Fann Instrument company. The two rheometers with springs F0.2 and F0.5 were delivered with two calibration fluids, respectively 20cP and 50cP viscosities. For the last rheometer with F1 spring, a calibration fluid of 100cP was used. For the rheometer to pass the check, the 300 and 600 rpm reading should give a value at the given temperature that is within ± 1,5cP the original viscosity from the calibration paper. Also the 600 rpm reading divided by 1.98 was compared to the chart value.

3.1 Fann® 35

The Fann® 35 viscometer is an instrument for measuring the rheological properties of both Newtonian and non-Newtonian fluids. The Fann® 35 is driven by a motor (1) in the back, as seen in Figure 7. This motor can be driven by two main gears by using the gear shift on the right hand side, but in this thesis only one gear was available. The steel cup (2) that comes with the rheometer were used only for the calibration fluid checks, during the rheologies of the other mixes, thermo cups were used. The red knob on top (3) is a secondary gear shift; this can operate while the motor is running unlike the other gear shift that require full stop. When the knob is down, 600 and 300 rpm is available, at top position; 200 and 100 rpm, and in a middle position; 6 and 3 rpm. Inside the cap (4) the torsion spring is located. The torsion springs react differently after how much torque they can handle. The measurement of this torque can be read off the reading dial (5). In the middle of the steel cup a cylinder (6) is located; this cylinder is a complete cylinder except from the access holes, where the fluid can move through freely. These access holes are the two small holes visible right next to the number 6 in the figure. The cylinder follows the movement of the motor, while the bob (7) is moved only by the fluid itself. The displacement of this bob is what will show on the reading dial, and how much it can endure is up to the sensitivity of the spring.

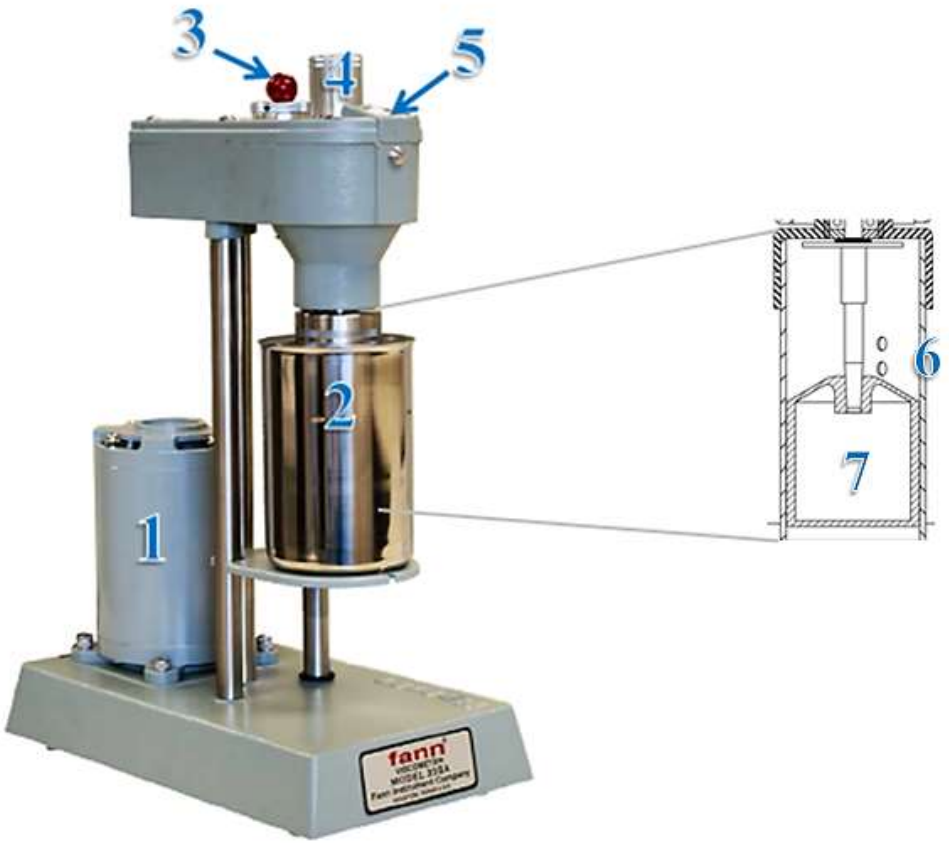

Figure 7 - Fann® 35 viscometer M35A – modified figure from Fann 35 Instruction Manual [6]

3.1.1 Lab tests

The rheometer used in this study is built to measure at six different speeds, from 600 rpm at the highest to 3 rpm at the lowest. The most common design of a Fann® 35 viscometer includes a B1 bob, R1 rotor sleeve and F1 torsion spring. There are possibilities of changing the rotor, bob and spring in several combinations to measure the rheology at other ranges, either by extending the torque measuring ranges or to increase the sensitivity of the instrument [6]. In this study the torsion springs F0.2 and F0.5 is applied in addition to F1, to broaden the shear stress ranges. The rheologies are measured at several temperatures to give an overview of how rheological features vary with different temperatures.

The Fann® 35 is a Couette rotational viscometer, which is explained already in section 2.3.2. A brief summary of the most important aspects will be given in this section: It has a bob inside the rotor sleeve leaving a small gap between the two, the shear gap or 'annular space'. When the rotor is circulating, it is giving a certain drag of the mud. The mud then creates a torque on the bob which can

be observed on the dial at the top of the rheometer. The results observed combined with the associated speed gives the consistency curve; shear rate versus shear stress [6].

The basic rheology is tested on a Fann® 35 rheometer with F1-spring at 50°C. In this thesis three Fann® 35 rheometers with different springs are applied. The springs are F0.2, F0.5 and F1, meaning the only differences of the viscometers are that the torsion springs are replaced in two of them. Figure 8 gives an impression of how to change the torsion spring on a Fann® 35 rheometer.

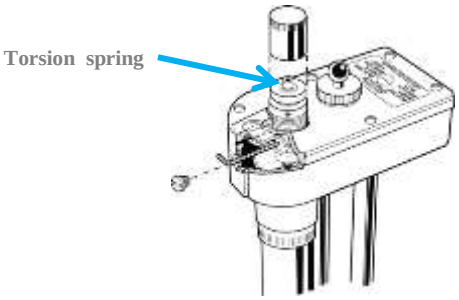

Figure 8 – The torsion spring location, edited figure from Fann® 35 Instruction Manual [6]

The six mixes were tested on every rheometer at three different temperatures: 25°C, 35°C and 50°C. The yield point YP and plastic viscosity PV can be calculated and added to the results if required. The plastic viscosity gives the slope of a straight line and it is based on the readings at 600 rpm and 300 rpm.

$$PV(cP) = \theta_{600} - \theta_{300} \qquad \textit{Equation 3-1}$$

While the yield point gives the theoretical point of where the straight line would intercept the vertical axis:

$$YP\left(\frac{lb}{ft^2}\right) = \theta_{300} - PV \qquad \textit{Equation 3-2}$$

These equations are exactly the same as Equation 2-20 and Equation 2-21 in section 2.3.2, but with different symbols.

3.1.2 Simulations

The method of the simulations is taken from the paper from Savins and Roper 1954[8] combined with the lecture note; "PET525 Drilling Automation – Exercise 1"[9] from the class of drilling automation at the University of Stavanger. Simulations were generated in MATLAB® to show the relationship between speeds in rpm (ω) versus dial readings (θ) and also shear rate (γ) versus shear stress (τ). The plots of the results from the viscometer are given by the simplified Reiner-Riwlin Equation 2-17, and when solving for the dial reading the equation looks like this:

$$\theta = \frac{\omega\mu_p + B\tau_0}{A} \qquad \textit{Equation 3-3}$$

Which gives a curve where the slope is $\frac{\mu_p}{A}$ and the intercept on the vertical axis is $\frac{B\tau_0}{A}$. The expression for the constant A is as followed;

$$A = K_s A_g \qquad \textit{Equation 3-4}$$

where K_s is the spring constant. This constant will vary through the several simulations as there are three different springs in the rheometers. The theoretical value of the F1 spring constant is 363 dyne-cm per deg. But as the table underneath shows, the spring constant of an F1 spring is set to 386 dyne-cm per deg, which is a correction for the bob end effects.

Torsion Springs			
F	**Constant**	**Max Shear Stress**	**Color Code**
F0.2	77.2	307	Green
F0.5	193	766	Yellow
F1	386	1,533	Blue
F2	772	3,066	Red
F3	1,158	4,600	Purple
F4	1,544	6,132	White
F5	1,930	7,665	Black
F10	3,860	15,330	Orange

Table 2 – Torsion spring constants, from "PET525 Drilling Automation – Exercise 1" [9]

The true value of the constant A is determined after calibrating the rheometer with a Newtonian fluid to see if there are any end effects of the bob-rotor design. What may vary is the A_g, which is the bob-rotor geometry constant defined by Savins 1954[8] and also by Kelessidis 2010[12], and is defined;

$$A_g = \frac{(100)(60)}{8\pi^2(L_b + L_e)}\left(\frac{1}{r_b^2} - \frac{1}{r_c^2}\right) \qquad \textit{Equation 3-5}$$

L_b is the length of the side of the bob, r_b is the radius of the bob and r_c is the radius of the cylinder. L_e is the correction factor. The constant B is given by

$$B = \frac{(100)(60)}{(0.208867)2\pi}\log_e \frac{r_c}{r_b} \qquad \textit{Equation 3-6}$$

Where 0.20886 is the factor used when converting dynes/cm^2 to lb/100ft^2. Calibration standards do not affect this constant meaning it will remain the same through the simulations.

The standard parameters of the Fann® 35 rheometer are as given in the table below; where"R_0" is the same as r_c, "R_i" is the r_b and "L" is the L_b. The values of these parameters at "R1 B1" are used in the simulation, the whole MATLAB® code is enclosed in Appendix B.

ROTOR-BOB	R1 B1	R2 B1	R3 B1	R1 B2	R1 B3	R1 B4
Rotor Radius, R_0 (cm)	1.8415	1.7588	2.5866	1.8415	1.8415	1.8415
Bob Radius, R_i (cm)	1.7245	1.7245	1.7245	1.2276	0.8622	0.8622
Bob Height, L (cm)	3.8	3.8	3.8	3.8	3.8	1.9
Shear Gap in Annulus (cm)	0.117	0.0343	0.8261	0.6139	0.9793	0.9793
Radii Ratio, R_i/R_0	0.9365	0.9805	0.667	0.666	0.468	0.468
Maximum Use Temperature (°C)	93	93	93	93	93	93
Minimum Use Temperature (°C)	0	0	0	0	0	0

Table 3 – The rotor and bob combinations and their associated constants [9]

In the simulations the viscosity is expressed;

$$\mu = \frac{\tau}{\gamma} = Kf\frac{\theta}{N} = \frac{100k_1k_2\theta}{Nk_3} \qquad \textit{Equation 3-7}$$

Where K is the total instrument constant, f is the spring constant also called k_1 or K_s in the MATLAB® code. 100 is the conversion factor between poise and centipoise, θ is the dial reading, N is the rate of revolutions of the outer cylinder and k_2 and k_3 is explained in Table 4.

Constant	Rotor-Bob Combinations					
	R1 B1	R2 B1	R3 B1	R1 B2	R1 B3	R1 B4
Overall Instrument Constant, K Standard F1 Torsion Spring $\eta = Kf\theta/N$	300	94.18	1355	2672	7620	15,200
Shear Rate Constant k_3, (sec^{-1} per rpm)	1.7023	5.4225	0.377	0.377	0.268	0.268
Shear Stress Constant for Effective Bob Surface k_2, (cm^{-3})	0.01323	0.01323	0.01323	0.0261	0.0529	0.106

Table 4 – The rotor and bob combinations with the overall instrument constant [9]

3.2 Dual DP

Previous work of Kurt Louis Krogsæter states that the Dual DP is a flow loop generated by students at the University of Stavanger. In 2011, Torsvik built a small scale drilling rig operated through a PC by using Simulink® – a modeling program. In 2012 Wang optimized the rig to a MPD rig and Hansen added the differential pressure transmitters. Finally, in 2013, Krogsæter expanded the application area of the data monitored; rheological parameters, friction factor and the density of the fluid were registered and plotted [10].

The flow loop has a horizontal pipe followed by a vertical pipe as illustrated in Figure 9. The loop is connected to a pump which drives the fluid flow through the system. On the loop there is a tank which holds the fluid; in this case water. If any other fluids were to be tested on this loop, it would have to be easy to clean, as particles may settle, or they may react with the tank etc. The several valves of the system connect the flow to the desired path. Two pressure monitors are mounted on the horizontal pipe; H1 and H2. Likewise on the vertical pipe there are two monitors; V1 and V2.

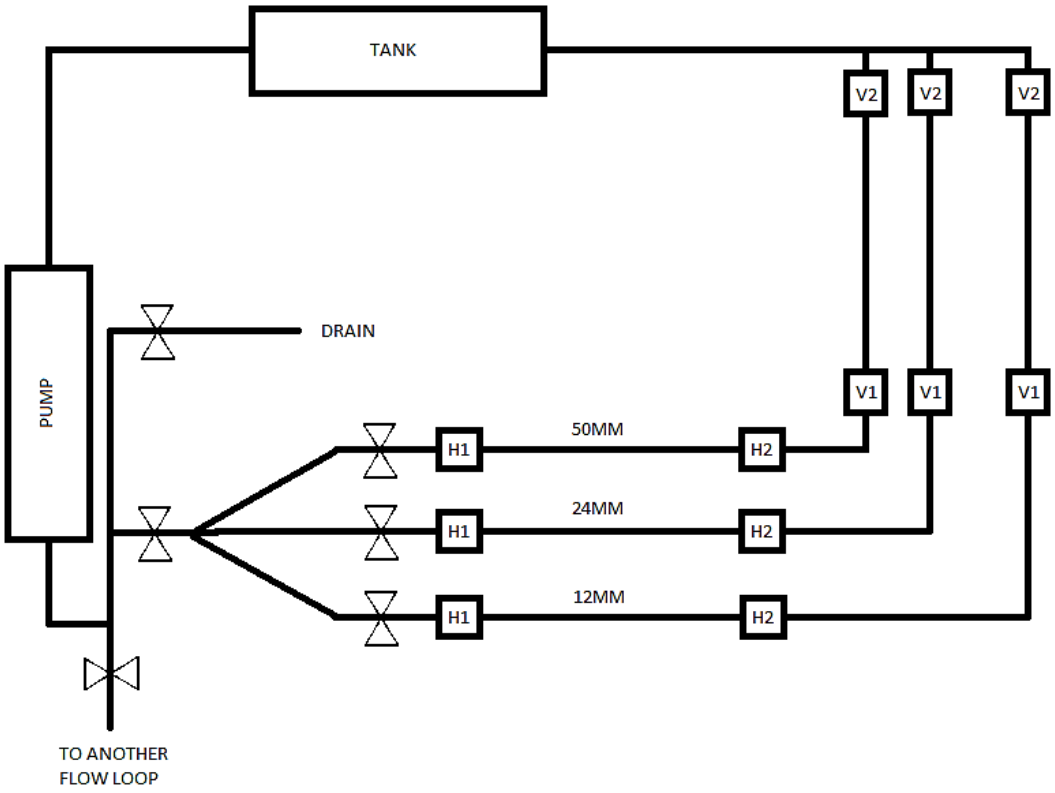

Figure 9 – Dual DP flow loop

The loop used in this thesis is the 24 mm loop, after examining the stability of Krogsæter's results [10]. By using Simulink® in MATLAB® the pump receives orders to either start or stop, in addition the pump rates can be set manually in this control window. When adjusting the pump rates they are chosen as a percentage of the maximum pump rate, which is 14 m^3/h. In this thesis the pump rates ranges from 0.1% to 0.35% with steps of 0.5%. To adjust from m^3/h to m^3/s and at the same time calculate the actual rate from the percentage, Equation 3-8 is applicable;

$$Q = \frac{pump\ rate\ \%\ \times 14}{3600} \qquad \textit{Equation 3-8}$$

The Dual DP testing were initiated by following the steps of Krogsæters "Operating Procedures", which is also found in Appendix A. In this thesis a total of six tests were performed, see Table 5.

Matlab name	Test1	Test2	Test3	Test4	Test5	Test6
Pump pressure % of maximum	0,1	0,15	0,2	0,25	0,3	0,35
Pump pressure m^3/s	0,000389	0,000583	0,000778	0,000972	0,001167	0,001361

Table 5 – Overview of the six tests performed and the coherent pump rate in % and m^3/s

The data from these tests were collected and compared. The plots generated from these data sets are based on differential pressure measurements the horizontal pipe, and from the vertical pipe. The most important and interesting properties; density and dynamic viscosity are plotted, in addition to the differential pressure itself, the friction factor and the Reynolds number.

Chapter 4 FANN® 35

This chapter contains the results of the tests regarding the rheologies tested on the Fann® 35 rheometer. The results are divided into two main groups; Simulations and Lab. The simulations of the calibration fluids were performed in MATLAB®. And the lab work was done at the fluids lab at the University of Stavanger.

4.1 Simulations

The simulations were performed with the intention of looking at the differences of the rheology data the calibration fluids reveals. There were in total nine simulations whose values are shown in Table 6. The calibration fluids are Newtonian, so the plot will show a line decreasing with speed.

Values calculated through simulations in MATLAB®									
Calibration	**Rheometer with F1**			**Rheometer with F0.5**			**Rheometer with F0.2**		
Viscosity	20 cP	50 cP	100 cP	20 cP	50 cP	100 cP	20 cP	50 cP	100 cP
600 rpm	40	100	200	80	200	400	200	500	1000
300 rpm	20	50	100	40	100	200	100	250	500
200 rpm	13,33	33,33	66,66	26,66	66,66	133,33	66,66	166,66	333
100 rpm	6,66	16,66	33,33	13,33	33,33	66,66	33,33	83,33	166,7
6 rpm	0,4	1	2	0,8	2	4	2	5	10
3 rpm	0,2	0,5	1	0,4	1	2	1	2,5	5

Table 6 – Values calculated through simulations in MATLAB®

In order to make these simulations, the base values for the MATLAB® code was needed. The calibration fluids were tested at the lab and entered at the "theta_Fann-real" in the code as seen in Appendix B. The gathered data from the rheologies are registered in Table 7.

Readings collected at the lab									
Calibration	**Rheometer with F1**			**Rheometer with F0.5**			**Rheometer with F0.2**		
Viscosity	20 cP	50 cP	100 cP	20 cP	50 cP	100 cP	20 cP	50 cP	100 cP
600 rpm	43,5	107	214,5	83	210	-	209	-	-
300 rpm	22,5	54,5	109,5	42	106	214	105	268	-
200 rpm	15	36,5	73,5	28	70,5	142	70	178,5	-
100 rpm	7,5	18,5	37	14	35,5	71	35,5	89,5	176
6 rpm	0,5	1,5	2,5	1	2	4,5	3	6	10,75
3 rpm	0,5	0,5	1,25	0,5	1	2,5	2	3,5	5,5

Table 7 – Calibration fluids tested in the lab, three fluids on three different rheometers

The differences between the simulated data and lab data were then compared in Table 8. The results in this table come from when values in Table 6 are subtracted from Table 7. These values of difference show that the experimental data does not coincide completely with the simulated data. The largest difference of the measurable data is with F0.2 at 300 rpm and the 50 cP fluid, but when looking at the lower speeds; 6 and 3 rpm the difference is not that great.

Difference									
Calibration	**Rheometer with F1**			**Rheometer with F0.5**			**Rheometer with F0.2**		
Viscosity	20 cP	50 cP	100 cP	20 cP	50 cP	100 cP	20 cP	50 cP	100 cP
600 rpm	3,5	7	14,5	3	10	-	9	-	-
300 rpm	2,5	4,5	9,5	2	6	14	5	18	-
200 rpm	1,67	3,17	6,84	1,34	3,84	8,67	3,34	11,84	-
100 rpm	0,84	1,84	3,67	0,67	2,17	4,34	2,17	6,17	9,3
6 rpm	0,1	0,5	0,5	0,2	0	0,5	1	1	0,75
3 rpm	0,3	0	0,25	0,1	0	0,5	1	1	0,5

Table 8 – The difference between simulation data and lab data

The rheometer with F1 spring was calibrated with a 100 cP calibration fluid, where θ_{300} is equal to the viscosity = 100 cP. The F0.5 spring was calibrated with a 50 cP fluid, but the θ_{300} is also showing 100. By dividing this with 2 it will be equal to the viscosity of the fluid. And likewise for the rheometer with F0.2 spring; it was calibrated with a 20 cP fluid, θ_{300} = 100; divide it by 5 and it equals the viscosity. By looking at the connections between the readings gathered from the three different rheometers, six equations have been generated. The connections made was that; if an F1 spring reading is 100%, then with the same fluid and a F0.5 spring which is 50 % more sensitive, the reading will increase accordingly. Likewise for the F0.2 spring which is five times more sensitive than the F1 spring, giving readings five times larger than at the standard conditions. The relationship between the readings collected by testing the same fluid at three different rheometers is as followed;

$$\theta_{F1,n} = \frac{\theta_{F0.5,n}}{2} = \frac{\theta_{F0.2,n}}{5} \qquad \textit{Equation 4-1}$$

where n is the speed of the rheometer. This connection further leads to equations that can be used to find readings across rheometers. From the rheometer with F0.2 spring, the expected value of the readings at the other two rheometers can be calculated at the equivalent speed.

$$\theta_{F0.5} = \frac{\theta_{F0.2} \times 2}{5} \qquad \textit{Equation 4-2}$$

When the standard is with the F1 spring the relationship between F0.2 and F0.5 is 2/5 in this case, and for the F1 spring;

$$\theta_{F1} = \frac{\theta_{F0.2}}{5}$$

Equation 4-3

For the rheometer with F0.5 spring the expected value at F0.2 is:

$$\theta_{F0.2} = \frac{\theta_{F0.5} \times 5}{2}$$

Equation 4-4

And to find F1 by the value of F0.5;

$$\theta_{F1} = \frac{\theta_{F0.5}}{2}$$

Equation 4-5

This is also possible to do the other way, if the F1 values are known and it is necessary to know what the expected value will be on a more sensitive spring. In example, the F0.2 and F0.5 has a maximum of torque they can handle, as shown in Table 7, there are some speeds left out in the rheology, this is due to the fact that the spring might burst if applied to such torque. The reading dial only goes up to 300, meaning all of the readings exceeding this value in Table 6 have not been tested on. To find the expected value of F0.2 from the values of F1;

$$\theta_{F0.2} = \theta_{F1} \times 5$$

Equation 4-6

And for the expected value of F0.5 from F1 values;

$$\theta_{F0.5} = \theta_{F1} \times 2$$

Equation 4-7

There are two plots for every calibration fluid; speeds in rpm versus dial readings and shear rate versus shear stress. In the plots the expected results calculated in MATLAB® is presented as blue rings and the measured results from the lab is presented as red rings. The whole MATLAB® code for these simulations is found in Appendix B. The constants used in these simulations are

Input data	Rc	Rb	Lb	Le	Ks-F0.2	Ks-F0.5	Ks-F1	k2	k3
Value	1,8415	1,7245	3,8	0,2451	77,2	193	386	0,01323	1,7023

Table 9 – Constants applied to the MATLAB® code

The K_s-values are only used one at the time relative to which one is simulated. The Herschel-Bulkley components are set to n = 1 and τ_0 = 0 for a Newtonian fluid. The K were selected after which fluid, 100 cP = 1, 50 cP = 0,5 and 20 cP = 0,2. The following plots are all simulated on a "regular" rheometer, which is with spring F1.

4.1.1 Calibration fluid – 100 centipoise

First the 100 cP calibration fluid was simulated. In Plot 1 the dial readings correlate very well at the beginning, at the higher speeds, but 6 and 3 rpm there are some apparent deviations. The deviation is 0,5 and 0,25 respectively, as seen in Table 8. But when studying the deviations of 600 and 300 rpm in the table; 14,5 and 9,5, the gap is much bigger. This is not showing in these plots as they are logarithmic. The simulations were also put in a shear rate versus shear stress plot, as the conversion from one plot to the other is fairly easy.

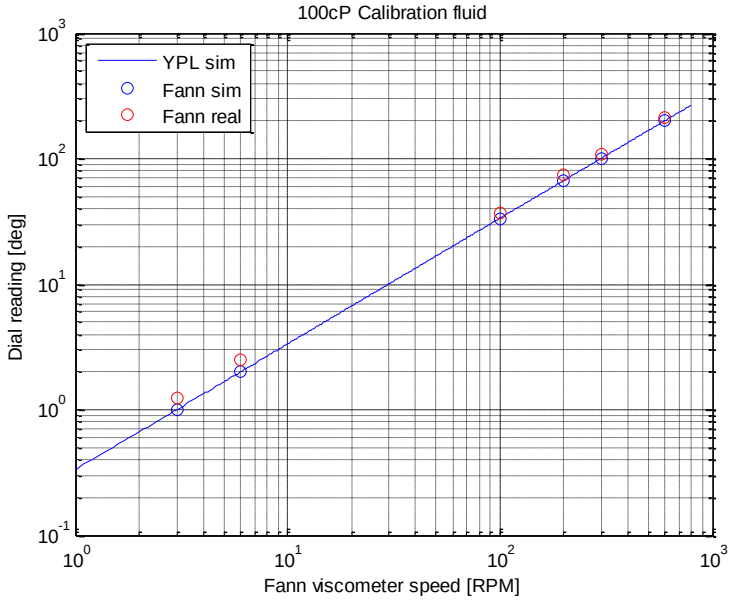

Plot 1 – 100 cP calibration fluid – Viscometer speed versus Dial reading

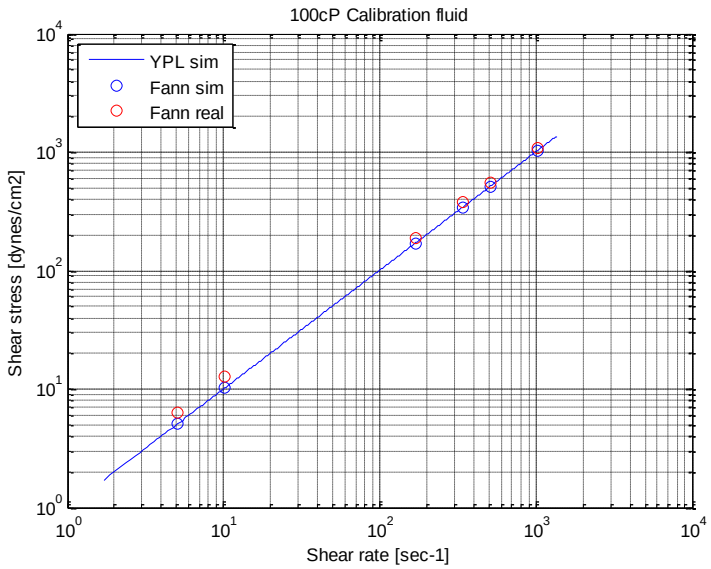

Plot 2 –100 cP calibration fluid – Shear rate versus Shear stress

4.1.2 Calibration fluid – 50 centipoise

The next simulation was the 50 cP calibration fluid on the rheometer with the F1 spring. The lab results are coinciding with the simulation, except for at 6 rpm. The deviation looks big, but it is only 0,5 rpm. The same point comes clear here, the lower the speed the less is needed for the deviation to stand out.

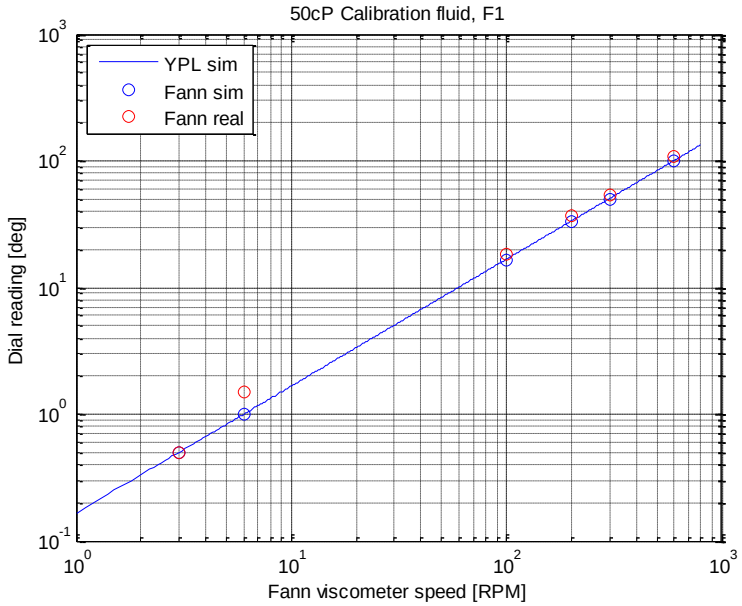

Plot 3 – 50 cP calibration fluid – Viscometer speed versus Dial reading

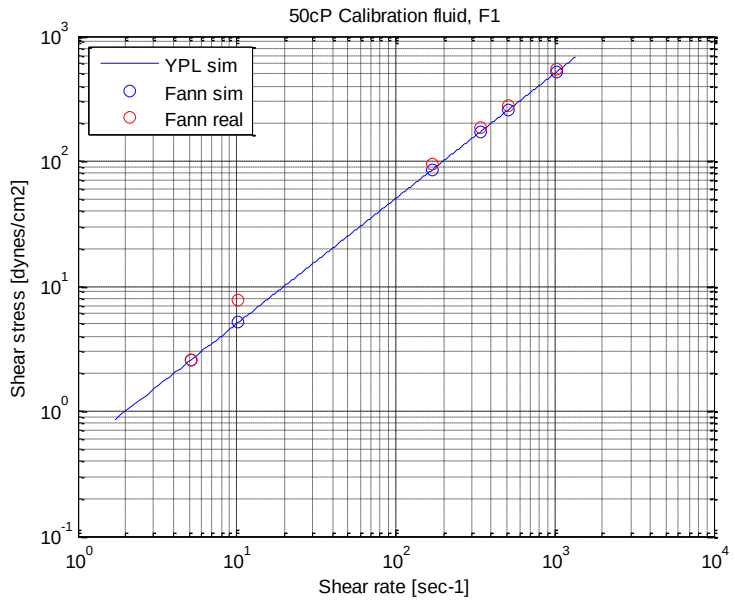

Plot 4 – 50 cP calibration fluid – Shear rate versus Shear stress

4.1.3 Calibration fluid – 20 centipoise

The last simulation was the 20 cP calibration fluid on the rheometer with F1 spring. The 6 and 3 rpm are showing simulated values of 0,4 and 0,2 respectively. The lab results give the same value on the two; 0,5.

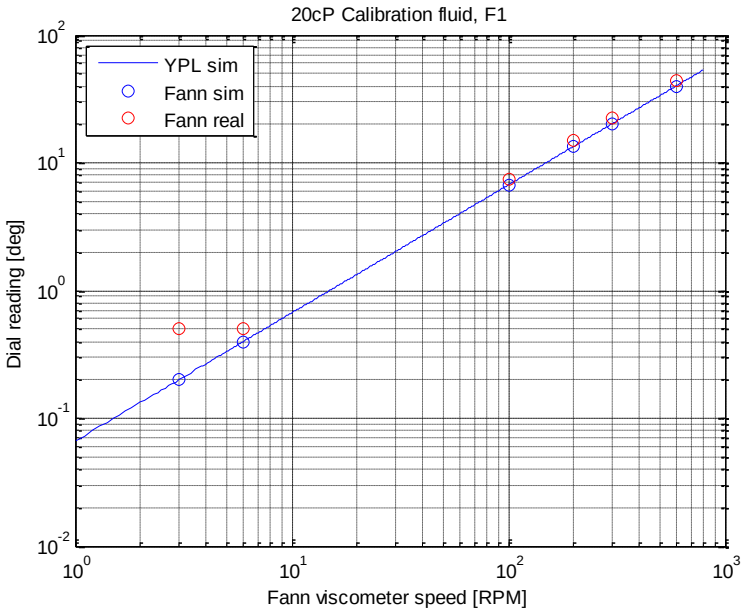

Plot 5 – 20 cP calibration fluid – Viscometer speed versus Dial reading

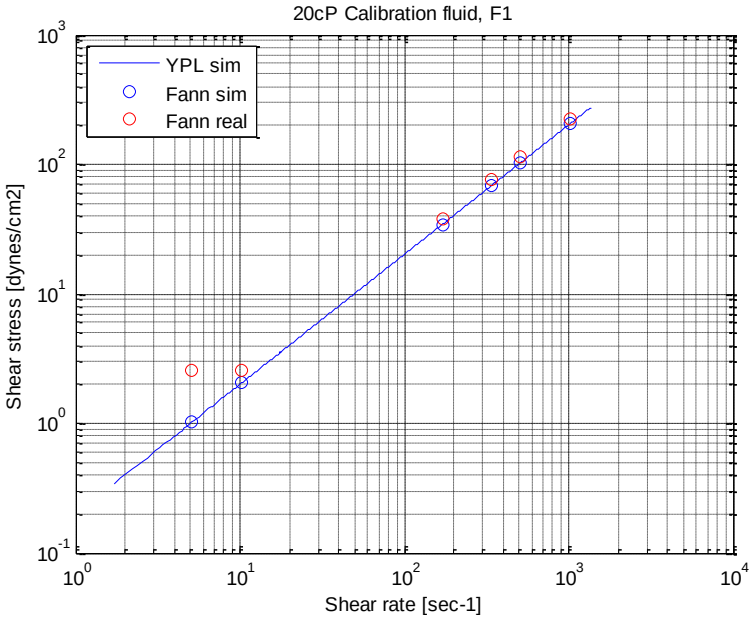

Plot 6 – 20 cP calibration fluid – Shear rate versus Shear stress

4.2 Lab

The lab tests were divided into two groups, first the calibration fluids were tested and then the six mixes were tested. The calibration fluids are of known viscosity and come with expected values, while the fluids mixed at the lab are unknown, and no calculations were performed prior to testing.

4.2.1 Calibration check

The rheometers were checked to see if the calibrations were good enough. The following values were read:

Calibration	F1	F0.5	F0.2
Viscosity	100 cP	50 cP	20 cP
Temp	21,6°C	21,6°C	21,7°C
600 rpm	207,5	207	200
300 rpm	106	104,5	101
200 rpm	71	69,5	67,5
100 rpm	36	34,5	34
Viscosity equals θ_{300}	106	52,25	20,2
Viscosity at given temp	103,1	51,8	20,2
Check at:	Deviation		
300 rpm	2,9	0,45	0
600 rpm	1,20	-0,05	-0,01

Table 10 – Calibration check results

The viscosity of the fluid is the value read at 300 rpm [6], which is checked at "Viscosity equals θ_{300}" in Table 10 – Calibration check result Below this line there is a "Viscosity at given temp"-slot, the values found here is the values from the sheet that comes along with the calibration fluid, the viscosity of the fluid is this noted value at the given temperature. The deviations show that for F1, the 300 rpm deviation was not within the limits of ±1,5 cP, but this might be because of the 100 cP fluid, which has not been checked on this rheometer before as it was sent separately. The rest of the calibration checks were all good. The two other calibration fluids were delivered together with the rheometers.

4.2.2 Lab tests

The six fluids mixed at the lab were all tested on the three different rheometers, at three different temperatures, leaving it to a total of 54 rheologies as displayed in Figure 10.

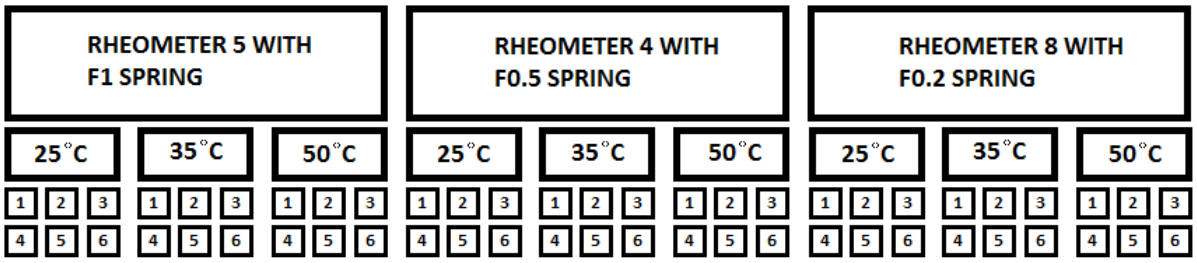

Figure 10 – Overview of the rheologies performed at the lab

The first mix was KCl brine with a specific gravity of 1,05 and 1 g/l DUOTEC NS. In Table 11 – Mix 1: 1.05 KCl brine with 1 g/L DUOTEC NSTable 11 it is clear that the viscosity is low. With rheometer 5 the viscosity is 4,5 at 24°C. By using Equation 4-3 and Equation 4-5 the new viscosities at the same temperature are 3,5 and 3,7 respectively, which is a bit lower than with the F1 spring. By looking at the whole rheologies at rheometer 5 they have a trend of decreasing the viscosity as the temperature increases, which is common for all the sets below. But when looking at the 6 rpm line at rheometer 5 the succession is 0,5 – 1 – 0,5. The viscosity acts differently as it goes from low to high and then low again. By looking at the same line, but at rheometer 8, the results are as expected, with a succession of 0,5 – 0,4 – 0,3 after converting to F1 spring.

Mix 1	RHEOMETER 5 WITH F 1			RHEOMETER 4 WITH F 0.5			RHEOMETER 8 WITH F 0.2		
Temperature (°C)	25	35	50	25	35	50	25	35	50
Measured temp (°C)	24	35	49,2	24,1	35,5	50,2	24,1	34,9	50,4
600 rpm	6,5	6	5	11	10	8,5	29	25,5	21
300 rpm	4,5	4	3	7	6,5	5,5	18,5	16,5	13
200 rpm	3,5	3	2,5	5,5	5	4,5	15	13	10
100 rpm	2,5	2	2	3,5	3,5	3	10	8,5	7
6 rpm	0,5	1	0,5	1	1	0,5	2,5	2	1,5
3 rpm	0,5	0,5	0,5	0,5	0,5	0,5	1,5	1,5	1

Table 11 – Mix 1: 1.05 KCl brine with 1 g/L DUOTEC NS

The next table is of a 1,05 KCl brine with 2 g/l DOU-TEC NS added. This table shows the same problem of low – high – low readings at rheometer 4 revealing that the uncertainty is still present, although the viscosifier amount is doubled. Again this problem is not visible with the F0.2 spring. One

thing is easy to spot in this table; at 3 rpm with rheometer 5 the results are 1 – 1 – 1, while there is a difference when tested with the F0.2 spring; 1 – 0,9 – 0,7 after the conversion.

Mix 2	RHEOMETER 5 WITH F 1			RHEOMETER 4 WITH F 0.5			RHEOMETER 8 WITH F 0.2		
Temperature (°C)	25	35	50	25	35	50	25	35	50
Measured temp (°C)	24,4	35,3	49,4	25,4	35,4	49,3	25,3	34	49,4
600 rpm	11	10	9	20,5	18,5	16,5	53,5	45	40
300 rpm	7	7	6	14	13	11,5	36	31,5	28
200 rpm	6,5	5,5	5	11	10,5	9,5	29,5	26	24
100 rpm	4,5	4	3,5	8	7,5	7	21	18,5	17,5
6 rpm	1,5	1,5	1	2	2,5	2	7	6	5
3 rpm	1	1	1	1,5	1,5	1	5	4,5	3,5

Table 12 – Mix 1: 1.05 KCl brine with 2 g/L DUOTEC NS

Table 13 is showing the results of mix 3; 1.05 KCl brine with 4 g/l DUO-TEC NS, the added amount is again doubled compared to the previous mix.

Mix 3	RHEOMETER 5 WITH F 1			RHEOMETER 4 WITH F 0.5			RHEOMETER 8 WITH F 0.2		
Temperature (°C)	25	35	50	25	35	50	25	35	50
Measured temp (°C)	24,1	35,8	49,3	25	34,3	49,1	25	34,4	49
600 rpm	23	21	19	44	40	37	108,5	98,5	89
300 rpm	17	15,5	14,5	32,5	30,5	28	81	73	67,5
200 rpm	14,5	13,5	12,5	27,5	25,5	24	68,5	61,5	57,5
100 rpm	11	10,5	9,5	20,5	20	18,5	52,5	47	44,5
6 rpm	5	4,5	4	9	8,5	8	22,5	19,5	18
3 rpm	4	3,5	3,5	7	7	6	18,5	16,5	14,5

Table 13 – Mix 1: 1.05 KCl brine with 4 g/L DUOTEC NS

The next three mixes are with 1.15 KCl brine. The increase in the specific gravity of the fluid is revealing minor changes in rheologies. In Table 14, mix 4 is showing similar rheology trends as mix 1, at 50°C on rheometer 5 the results are all the same except for 6 rpm. But, when looking at the rest of the results there seem to be a decrease in rheology.

Mix 4	RHEOMETER 5 WITH F 1			RHEOMETER 4 WITH F 0.5			RHEOMETER 8 WITH F 0.2		
Temperature (°C)	25	35	50	25	35	50	25	35	50
Measured temp (°C)	24,4	35,6	49,6	25,2	35	49,7	24,7	34,8	49
600 rpm	6	5,5	5	11	9,5	8,5	28,5	23	20,5
300 rpm	4	3,5	3	7	6	5,5	17,5	15	13
200 rpm	3	3	2,5	5	4,5	4	14	11,5	10
100 rpm	2	2	2	3	3	2,5	9,5	7,5	6,5
6 rpm	0,5	0,5	1	0,5	0,5	0,5	2,5	2	1,5
3 rpm	0,5	0,5	0,5	0,5	0,5	0,5	2	1	1

Table 14 – Mix 1: 1.15 KCl brine with 1 g/L DUOTEC NS

Mix 5 can be compared to mix 2, due to the same amount of DUOTEC NS added. The changes are very small, with rheometer 5 the results are overall similar. Again with rheometer 8 the differences are bigger, but the thing that stands out here is that the rheology measured is actually lower with an increased SG, here it is around 3 dial readings lower than before.

Mix 5	RHEOMETER 5 WITH F 1			RHEOMETER 4 WITH F 0.5			RHEOMETER 8 WITH F 0.2		
Temperature (°C)	25	35	50	25	35	50	25	35	50
Measured temp (°C)	25,6	35,6	49	24,4	36	49,1	24,7	34,8	49,3
600 rpm	10,5	10	8,5	19,5	18	17	49,5	42,5	39
300 rpm	7	7	6	13	12,5	11,5	35,5	29	27,5
200 rpm	5,5	5,5	5	11,5	10	9,5	29	23,5	22
100 rpm	4	4	3,5	7,5	7	7	20,5	16	15
6 rpm	1,5	1,5	1	2	2	2	6	5	4
3 rpm	1	1	1	1,5	1	1,5	5	3,5	3

Table 15 – Mix 1: 1.15 KCl brine with 2 g/L DUOTEC NS

The last mix was a mix of 1.15 KCl brine combined with 4 g/l DUO-TEC NS. Here the patterns are as expected with an increase in SG; the viscosity of the fluid is higher. The increase is very small, about 0.5 dial readings for rheometer 5.

Mix 6	RHEOMETER 5 WITH F 1			RHEOMETER 4 WITH F 0.5			RHEOMETER 8 WITH F 0.2		
Temperature (°C)	25	35	50	25	35	50	25	35	50
Measured temp (°C)	24,1	35,5	49,7	25	35,3	49,5	25,5	34,1	50,6
600 rpm	23,5	21,5	19,5	44,5	41,5	38,5	112	100,5	92
300 rpm	17,5	16	15	33	31	29	83	75	70
200 rpm	14,5	13,5	12,5	28	26,5	25	70	63	59
100 rpm	11	10,5	9,5	20,5	20	19	53	48	45,5
6 rpm	5,5	5	4	9	8,5	8	23	20	19
3 rpm	4	4	3,5	7	7	6,5	20,5	17	15

Table 16 – Mix 1: 1.15 KCl brine with 4 g/L DUOTEC NS

4.3 Discussion

The interesting part about the calibration fluid simulations was to see if the rheologies tested with an F0.2 spring were better than the rheologies tested with an F1spring at 6 and 3 rpm. For these values to be comparable the values of F0.2 would have to be five times higher than the value read on the dial, as the spring is five times more sensitive; 0.2 to 1. This is where the equations in section 4.1 come in. The equations are generated to give an expected value of what a certain dial reading would be by applying a spring with different sensitivity. In example; in Table 7 the rheometer with F0.2 spring and 100 cP calibration fluid has a value of $\theta_{6,F0.2}$ = 10.75 for the 6 rpm reading, while the reading at the rheometer with F1 spring is $\theta_{6,F1}$ = 2.5. By using Equation 4-3, the calculated value of the 6 rpm reading at F1 is: $\theta_{6,F1,calc}$ = 10.75/5 = 2.15. This value is close to 2.5, but it is even closer to 2. This can suggest that the readings of the F0.2 rheometer will give a more precise number at lower speeds, as the simulated value was 2.

There are three tables in section 4.1; Table 6 – Values calculated through simulations in MATLAB®, Table 7 – Calibration fluids tested in the lab, three fluids on three different rheometers and Table 8 – The difference between simulation data and lab data. When looking at the differences in Table 8 – The difference between simulation data and lab data, the values vary, but in a controlled way. The greater the viscosity is the more it differs, and also by increasing the speed the difference will increase. At the lower speeds of 6 and 3 rpm, the differences are not that big, and these are the most interesting numbers as they reflect what happens in the annulus. The deviations at these speeds can be very small, but might matter a great deal in the big picture. So the question is; can this regular Fann® 35 be improved so that these numbers are more certain? The greater torque experienced by the spring the greater climb the dial read will have. The F0.2 rheometer will give better results, as the dial reading range is widened and the readings are easier to collect in general. After experience, there is a big uncertainty from 0 to 5 on the dial, as the impact is so small on a scale that seems to be unsuitable for giving proper readings. Also, at some occasions, the pointer showing the dial number might be slightly below zero, making a reading go from actually being 3.5 to 3. This problem will also be smaller as the deviation gap from zero will be divided by 5 automatically when applying the equations.

The data of the calibration fluids were then used to make plots of the simulated and lab data. The plots revealed a pattern where the deviations at the lower speeds looked larger than at the higher speeds. Although, Table 17 below shows it differently, this table shows the percentage of deviation from the simulated value. The deviations are almost constant when looking at the percentage, but it is actually higher at the lower speeds, which the plots also reveal. When looking at the table, there are four marked values at the 100 cP calibration fluid rheologies; they are at the 6 and 3 rpm with the F1- and F0.2 spring. It is obvious in this case that using the F0.2 for these values are better. The lower

deviation percentage might indicate that the uncertainty of the dial readings decreases as the range of impact increases.

% deviation									
Calibration	**Rheometer with F1**			**Rheometer with F0.5**			**Rheometer with F0.2**		
Viscosity	20 cP	50 cP	100 cP	20 cP	50 cP	100 cP	20 cP	50 cP	100 cP
600 rpm	0,088	0,070	0,073	0,038	0,050	-	0,045	-	-
300 rpm	0,125	0,090	0,095	0,050	0,060	0,070	0,050	0,072	-
200 rpm	0,125	0,095	0,103	0,050	0,058	0,065	0,050	0,071	-
100 rpm	0,126	0,110	0,110	0,050	0,065	0,065	0,065	0,074	0,056
6 rpm	0,250	0,500	**0,250**	0,250	0,000	0,125	0,500	0,200	**0,075**
3 rpm	1,500	0,000	**0,250**	0,250	0,000	0,250	1,000	0,400	**0,100**

Table 17 – Percentage of deviation from the simulated value

Several of the readings collected at the lab show the same results for 6 and 3 rpm, which is incorrect according to the theory. There *is* a difference of these readings, but the equipment is not good enough to separate them. The human eye can only see and evaluate to a certain degree, in addition to a reading dial that only has marks for every whole number. An idea would be to change the dial, and make it easier to use. The dial could have marks for every half number, especially from 0 to 5. Or to get the dial closer to the reading window, by looking with one eye first and then the other, there is a difference of one or two dial reading points. This would be easier than giving every rheology tester directions to stand in a certain position and looking with the same eye. Another idea might be to use the rheometer with the F0.2 spring for the low speeds, and calculate it back to the value it would give with an F1 spring, which would be much easier than changing the whole setup of the equipment.

In the tables of all the rheologies performed at the lab, Table 11 to Table 16, a few characteristics of the most common rheology test were revealed. There were successions showing low – high – low as the testing temperature increased. The expected behavior is high – lower – lowest, viscosity changes with temperature and there will be a reduction of the resistance in the fluid as the temperature increases. The error regarding this matter might occur when collecting the readings, which further means that there is a big uncertainty in the reading results that are collected by the human eye.

The rheologies were compared in pairs of how much DOU-TEC NS was added to the mixes. Mix 1 and 4 had 1 g/l viscosifier added to the brine; the dial readings of mix 4 revealed a lower rheology than mix 1. The first thought would be that as a fluid becomes heavier it should also give more resistance to movement, which clearly is not the case here. The same goes for mix 2 compared to mix 5 with 2 g/l of viscosifier; they show the same pattern with a decrease in viscosity. For the last two mixes; mix 3 and 6, the pattern has changed; there is an increase in the patterns of the rheologies, meaning the thought might be true for some combinations of weight versus viscosity.

Chapter 5 DUAL DP

The Dual DP tests were performed at the fluid flow lab at the University of Stavanger. There were some test runs prior to the actual tests to see if the system functioned as expected. When test runs were approved, the six main tests were performed. The data from these tests were extracted from the computer and plots were generated through Simulink® in MATLAB®. The plots have been divided into four groups; differential pressure, density, dynamic viscosity and friction factor together with the Reynolds number. The recommendation from Krogsæter [10] that the pump rate should not exceed 0.2% of maximum rate, was discovered too late. There are some rates exceeding this value, giving results that go above 100 mBar, which is not visible in these plots as the readings stop at this point.

5.1 Differential pressure

The differential pressure readings are the basis of the calculations of the rest of the values. It is therefore important that these readings are good, if not, it would affect the other plots to a certain degree. The differential pressure measured in the horizontal pipe is presented in Plot 7. The readings were good as all of the readings have smooth lines with the same trend; they show an increased value of differential pressure as pump rate increases, which is as expected. The time frame of the tests were from 0s to somewhere in between 130-160s.

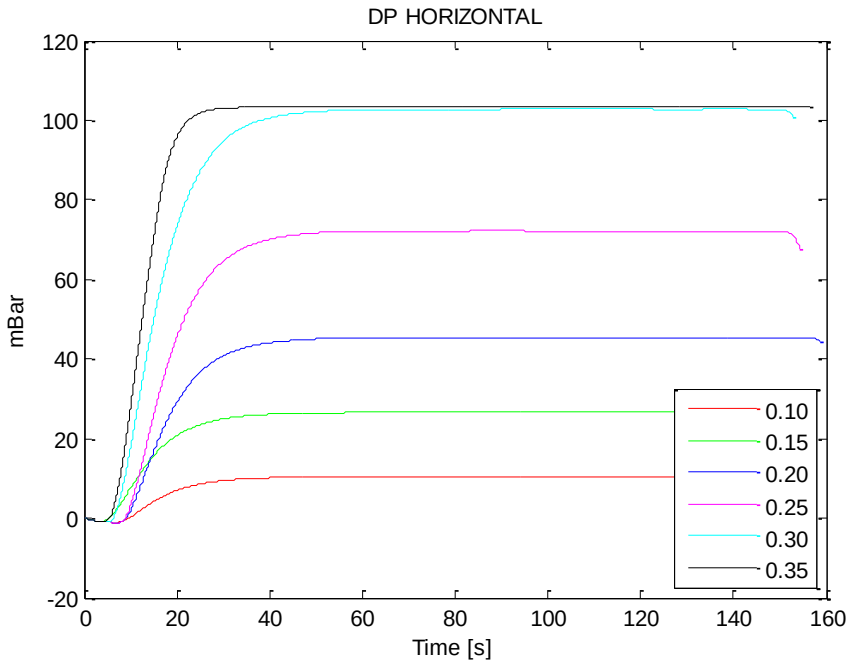

Plot 7 – Differential pressure in the horizontal pipe, mBar versus time in seconds

The differential pressure of the vertical pipe is displayed in Plot 11Plot 8. The results are still good, meaning all of the sensors work as they should. The 0.15, 0.20 and 0.25 show a different trend in the beginning of the measurements. The differential pressure readings here are somewhat higher than in the horizontal section.

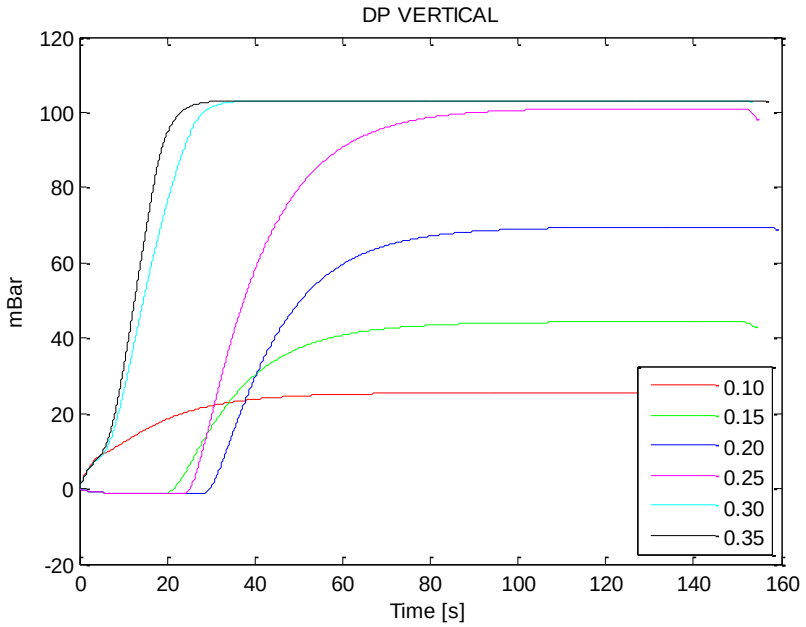

Plot 8 – Differential pressure in the vertical pipe, mBar versus time in seconds

Plot 9 and Plot 10 is showing the basis of the previous plots. The voltage readings are collected directly from the pressure sensors and are recalculated to the pressure unit mBar. It is clear that the trends of the readings in these plots are similar to the trends of the lines in the previous plots; Plot 7 and Plot 8.

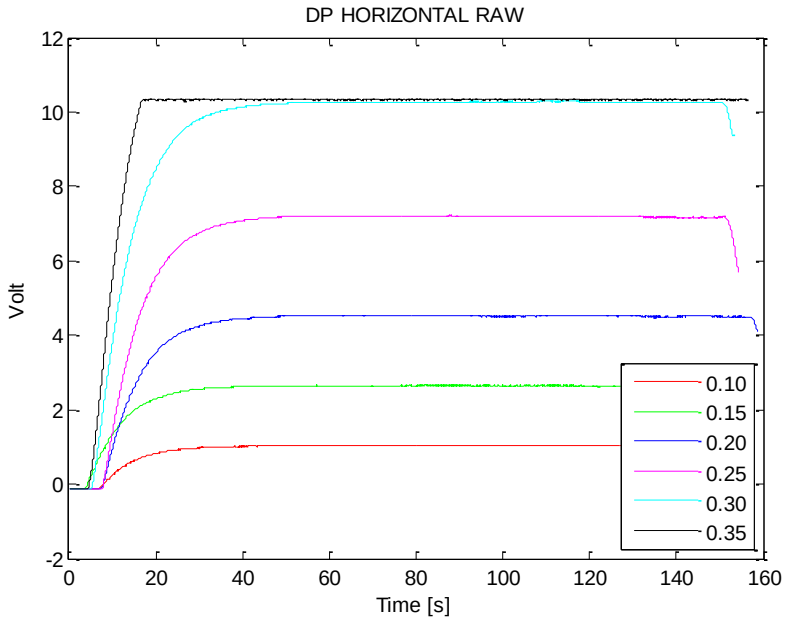

Plot 9 – Voltage readings in the horizontal pipe, volt versus time in seconds

The voltage readings of the vertical section are showing an initial value of 1 volt for the 0.10, 0.30 and 0.35 rates.

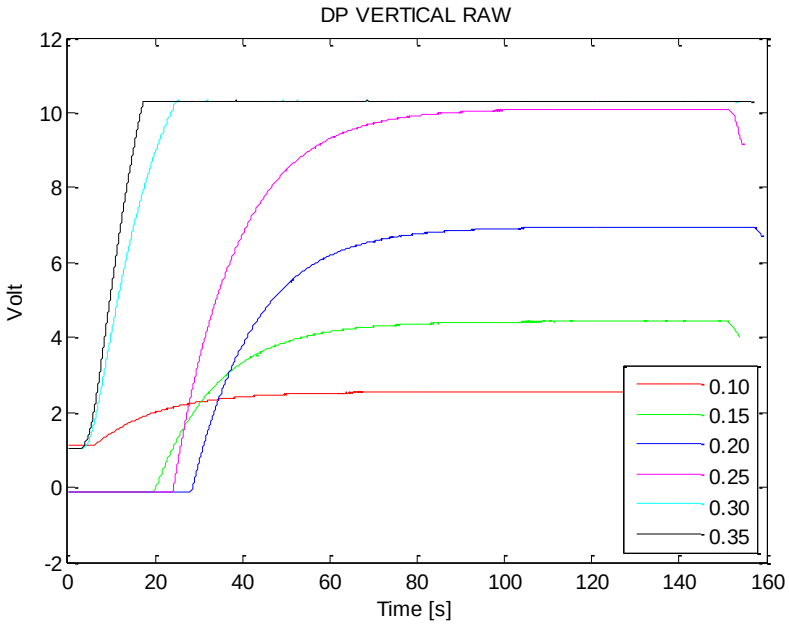

Plot 10 – Voltage readings in the vertical pipe, volt versus time in seconds

At last there is a plot with both horizontal and vertical readings. Here it is clear that the vertical section has a bigger differential pressure than the horizontal. The difference of horizontal and vertical pipes is marked with an H for the horizontal differential pressure readings. The best results of these tests are the 0.10, 0.15, 0.20 and maybe the 0.25, as the two last readings go out of the pressure window of 100 mBar.

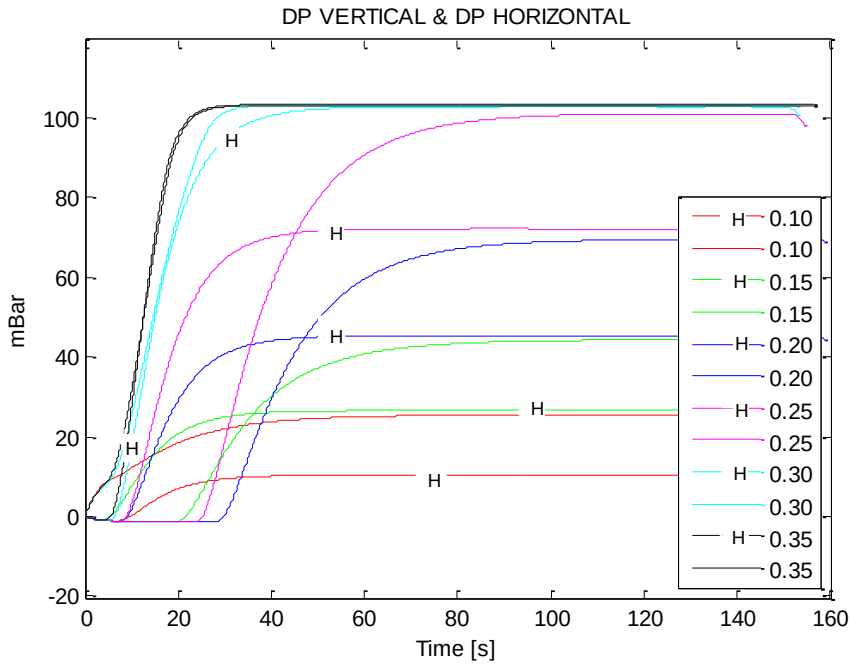

Plot 11 – Differential pressure in the horizontal- and vertical pipe, mBar versus time in seconds

5.2 Density

The density is displayed in Plot 12. Every density curve has an irregular trend at the beginning of the test. Some straighten out faster than the others within 30 s, while others are linear at 110 s at the earliest. The densities vary within the density range of 950 to 1050 kg/m^3. The density of water is around 998 kg/m^3 at 20°C, which is the approximate temperature of the lab. The first and second reading show results closest to this value. The following two show values that are much higher than the theoretical density of water, while the two with highest pump pressure rate show a density that is lower.

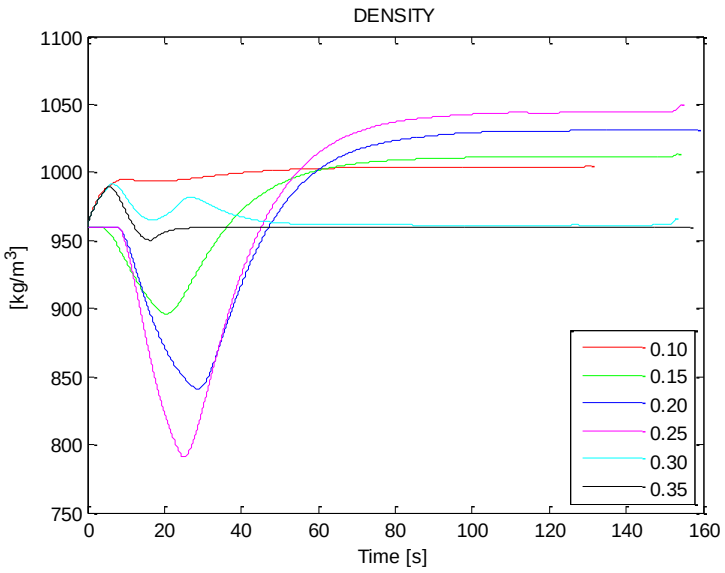

Plot 12 – Density in kg/m^3 versus time in seconds

5.3 Dynamic viscosity

The dynamic viscosity readings vary from 0.0003 to 0.0018 kg/m*s, but the 0.30 and 0.35 pump rates should probably be excluded in this plot as well. The new variation is from 0.0003 to 0.0012 kg/m*s.

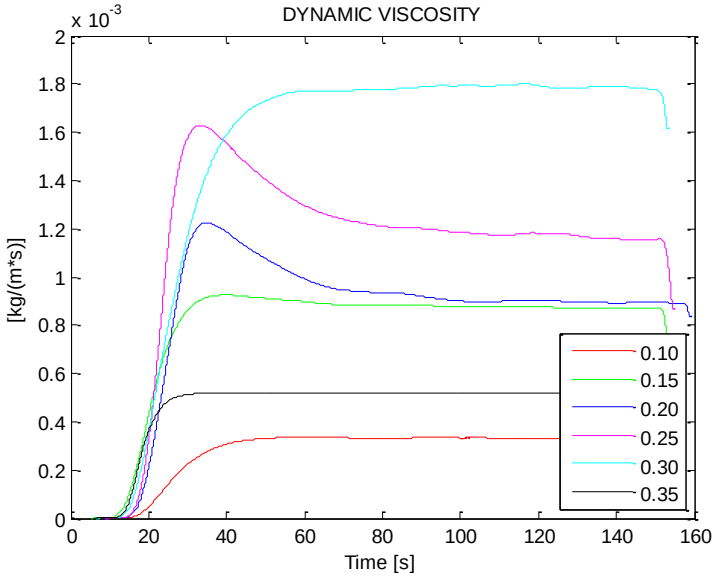

Plot 13 – Dynamic viscosity in kg/m*s versus time in seconds

5.4 Friction factor and Reynolds number

The friction factor readings vary within the range 0.015 to 0.025 with the average weight around 0.022 as displayed in Plot 14.

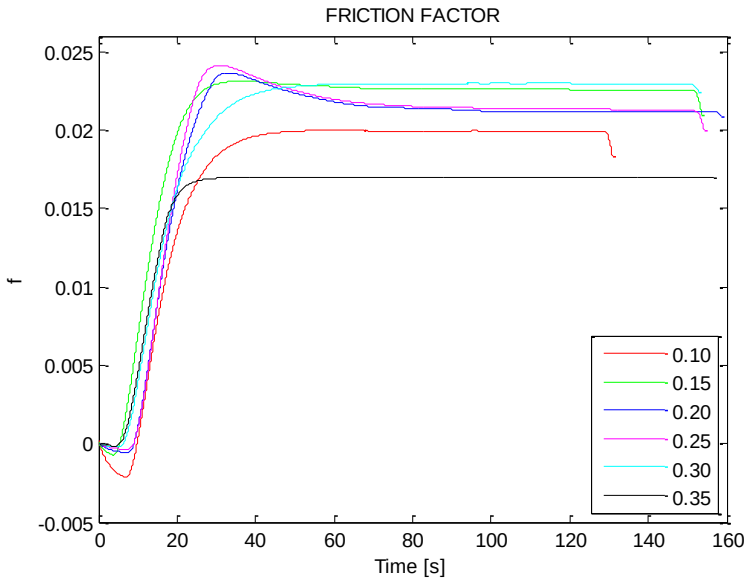

Plot 14 – Friction factor f versus time in seconds

The Reynolds number readings give the opposite trends of the friction factor readings, which is as expected. The weighted mean here is just above 0.4.

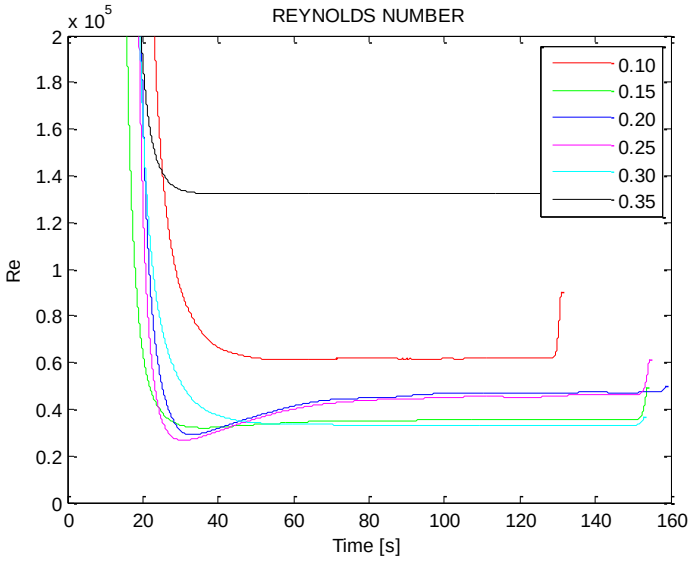

Plot 15 – Reynolds number Re versus time in seconds

5.5 Discussion

The differential pressure readings in the vertical section were consistently higher than at the horizontal section, which is not that odd as the gravitational force has a bigger impact on the system at this point, causing a larger pressure loss in the vertical system. The tests readings exceeding the 0 – 100 mBar range should be excluded. Later testers of the Dual DP system should be aware that, before executing the tests, the pump rate percentage of maximum pump rate should not exceed 0.2.

The density readings of the fluid in the system vary as the tests are carried out. Test 1 and 2 gave fairly good readings of the density, which is located around the theoretical value of water density. Test 3 and 4 were too high and test 5 and 6 were too low. Krogsæter also experienced the same problem in his thesis and looked more into the reasons why this might be. The deviations from theoretical value might be because of the density of the oil in the diaphragms. The density of the oil is said to be 960 kg/m^3 according to the supplier of the diaphragms. Krogsæter's theory is that if the density of the oil is changed, the calculations give the theoretically correct values of the density readings [10]. This can also be checked according to these results as well. Test 5 and 6 might have some uncertainty connected to the density values as the differential pressure readings are restricted to the range 0 - 100 mBar, and both of these tests exceeded the limits of this range.

Chapter 6 A review of the economic benefits

This chapter will look at the economic consequences of automating the drilling fluid analysis on an offshore installation, and its following benefits.

Today there are new ways of thinking relative to how it is possible to automate the drilling fluid evaluation in a drilling operation facility. These new ways are really worth having a look at, not just because it is an easier process, but because it can increase the precision of the evaluation and lower the overall costs. When testing drilling fluid manually there is a bigger imprecision in the work that is performed, compared to what an automated system would yield. There is also a big benefit of this new change when looking at personnel safety; the engineer would no longer be exposed to the chemicals and other hazards. Also, with an automated drilling mud system the mud would be of a better quality as the precision of added chemicals is much greater.

Field trials of automated mud mixing systems have been performed on the Valhall installation. The trials show an easier technical process as well as a more efficient drilling operation. Stability was also a product of this change as the margin of errors were smaller when there were no humans executing the work, and at the same time the chemical exposure where reduced significantly. Some of the positive feedback from operators of Valhall is that by having an automatic circulation on mud pits, it is easier to get a better overview from the control room. Another positive feedback is that it reduces risk combined with overfilling the mud pits, as the automatic system gives a more precise implantation of the process.

The ability of being able to perform all the operations associated with the drilling mud process in a control room, instead of actually performing the actions manually, is a system that is appreciated by the users. The stress of being exposed to hazardous chemicals and working in confined spaces nearly evaporates as the automated system does the job.

The consequences of changing the drilling fluid testing system from manually to automatically, result in an overall reduced environmental impact and at the same time it is cost efficient when looking at the reduced manpower needed. The drilling mud system is also safer and more reliable at the same time as the mixing process is more efficient [2].

Chapter 7 Summary and further study

The Fann® 35 tests were successful and gave good values, which can be of use to future workers within the field. Equations making it possible to calculate across the spring sensitivities were generated and functioned as a converter between the different readings. An improvement to the basic rheology test on the Fann® 35 viscometer will surely be to use the F0.2 spring to collect the 6 and 3 rpm readings, when the viscosity of the fluid is within F0.2's torque limits. The readings here were easier to collect when testing at the lower speeds, and the uncertainty level of the one performing the tests was also reduced giving a greater satisfaction with the collected results. The errors entered in the mud report will be smaller and the following consequences less severe. Further tests should be executed to confirm this. A possibility is to expand the fluid contents and make a complete mix; the test should verify the results.

Another potentially important thing is the measurement accuracy of the tests with the three different springs. While collecting the readings the tester should look at minimum and maximum values as well as the values collected at standard conditions. These three values should be plotted together to see how the misread deviations act along the decreasing profile of the rheometer speed. This measurement precision can further be included in the pressure loss calculations; the original data here should also be plotted in with minimum and maximum pressure fall as a combination of the three.

The Dual DP system is highly functional; the process can be executed easily by following "Operating Procedures" taken from Krogsæter 2013 [10], which is found in Appendix A. The next step with the Dual DP system is to run this loop with the non-Newtonian fluid created in the lab; a KCl brine with DUO-TEC NS. Before executing the tests, the tester should keep in mind that the system has a maximum pump rate that should not be exceeded. The new maximum pump rate should be calculated in accordance to the properties of the new fluid going through the system.

There are only positive consequences of an automated drilling mud system so far from an economic view; it will lead to better process efficiency and reduction in manpower, meaning an overall reduction in the associated costs. Continuing the research of better ways to execute the whole drilling fluid evaluation process is recommended. There should also be a further study of the cost benefit analysis of this subject on a more thorough level, to see if the current prognosis is applicable for all facilities.

Appendix A

Dual DP operating procedure

Taken from Krogsæter 2013 [10].

Operating Procedures

Startup

1. Ensure the tank is filled up with liquid.
2. Close the valve connected to the other flow loop.
3. Close all valves related to the Circulation Path.
4. Mount the diaphragms at desired pipe diameter.
5. Open valve to the pipe diameter selected.
6. Ensure all extension cords are connected.
7. Run "datafil" in Matlab.
8. Start up "difftest" in Simulink.
9. Select correct pipe diameter in Simulink - /maling/Subsystem4.
10. Compile and connect to target.
11. Start the process with preferred settings.
12. Run until a stable flow have been reached

Shutdown

1. Stop the system.
2. Drain the water from the Circulation Path.
3. Open all valves.
4. Unplug extension cords.
5. Extract data from Matlab.
6. Shut down computer.
7. Clean up potential spills.

Appendix B

MATLAB® **code**

Taken from "PET525 – Drilling Automation – Exercise 1 Solution"[13]

```
%Solution Exercise 1
close all;
clear all;
%To run the example, first create some random data to fit.
%The following commands create random data that is approximately
%exponential with parameters A = 40 and lambda = .5.

xdata = [3;6;100;200;300;600]';


%% Fann 35 data

% Defining instrument constants for Fann 35
r_c = 1.8415;
r_b = 1.7245;
l_b = 3.8;
l_e = 0.2451; %Correction factor according to Savins 1954 , Kelessidis 2010
%K_s = 77.2; %F0.2
%K_s = 193; %F0.5
K_s = 386; %F1
%K_s = 363; %F1 theoretical giving A = 300
k1 = K_s; % torsion constant
%k1 = 363; % torsion constant (theoretical)
k2 = 0.01323; % shear stress constant for bob surface
k3 = 1.7023;

% k1*k2 = dial2stress = 5.11;


% defining instrument constant A
% using Eq 6 and Eq 7
A_g = ((100*60)/(8*pi*pi*(l_b+l_e)))*((1/(r_b*r_b))-(1/(r_c*r_c)));
A = K_s* A_g;

% defining instrument constant B
% using Eq 11
B = ((100*60)/(0.20886*2*pi))*log(r_c/r_b);
%B = ((100*60)/(0.20886*2*pi))*log(r_c/r_b);


%% Simulating Fann35

theta_Fann_real = [1.25;2.5;37;73.5;109.5;214.5]'; % Read by Nina 100cP
mudtype = '100cP Calibration fluid';
%theta_Fann_real = [0.5;1.5;18;35.5;53;104]'; % Read by Nina 50cP, på F1
%mudtype = '50cP Calibration fluid, F1';
%theta_Fann_real = [0.5;0.5;7;14;21;41.5]'; % Read by Nina 20cP, på F1
%mudtype = '20cP Calibration fluid, F1';

% Herchel -Bulkley parameters
tau_0 =    0;
K =    1; % 1P = 100cP
%K =    0.5; % 0.5P = 50cP
%K =    0.2; % 0.2P = 20cP
n =    1; % Newtonian fluid
```

```
tau_0_pp100ft = tau_0*0.20886;
omega_rpm = [1:0.1:800];
omega_rpm_Fann = [3;6;100;200;300;600];

gamma = k3*omega_rpm;
gamma_Fann = k3*omega_rpm_Fann;

tau = tau_0 + K.*(gamma).^n;
tau_Fann = tau_0 + K.*(gamma_Fann).^n;
tau_dial = k1*k2*theta_Fann_real;

my_p_P = (tau-tau_0)./gamma; % in poise
my_p_P_Fann = (tau_Fann-tau_0)./gamma_Fann; % in poise
my_p_cP = 100*my_p_P; % centiPoise [cP]
my_p_cP_Fann = 100*my_p_P_Fann; % centiPoise [cP]
theta = (my_p_cP.*omega_rpm)/A + (B*tau_0_pp100ft)/A;
theta_Fann = (my_p_cP_Fann.*omega_rpm_Fann)/A + (B*tau_0_pp100ft)/A;

figure;
loglog(omega_rpm,theta,'b',omega_rpm_Fann,theta_Fann,'bo',omega_rpm_Fann,theta_Fann
_real,'ro')
ylabel('Dial reading [deg]');
xlabel('Fann viscometer speed [RPM]');
title(mudtype);
legend('YPL sim','Fann sim','Fann real','Location','NorthWest');
grid on;
disp(omega_rpm_Fann');
disp(theta_Fann');

figure;
loglog(gamma,tau,'b',gamma_Fann,tau_Fann,'bo',gamma_Fann,tau_dial,'ro')
ylabel('Shear stress [dynes/cm2]');
xlabel('Shear rate [sec-1]');
title(mudtype);
legend('YPL sim','Fann sim','Fann real','Location','NorthWest');
grid on;

% figure;
% loglog(gamma,tau,'b',gamma_Fann,tau_Fann,'g',gamma_Fann,tau_dial,'ro')
% ylabel('Shear stress [dynes/cm2]');
% xlabel('Shear rate [sec-1]');
% title(mudtype);
% legend('YPL sim','Fann sim','Fann real');
% grid on;
%
```

References

[1] B. Bloys, N. Davis, B. Smolen, L. Bailey, L. Fraser, M. Hodder, "Designing and Managing Drilling Fluid" (1994). http://www.slb.com/~/media/Files/resources/oilfield_review/ors94/0494/p33_43.pdf

[2] J. Gunnerød, S. Serra, M. Palacios-Ticas, "Highly automated drilling fluids system improves HSE and efficiency, reduces personnel needs", (2009).

[3] C. Radin, "Main Pump Start-up Pressure Limitation Control System when using Thixotropic Drilling Fluids", University of Stavanger, (2013).

[4] G. Nygaard, E. Cimpan, "Simulation and Evaluation of the Drilling Fluid Mixing and Conditioning Process", Bergen University College, (2013), p 76-86.

[5] Halliburton, "Fann Product Catalog", (2014), p 8. http://www.halliburton.com/public1//pubsdata/Overview/Doc_Showcase/catalog_web.pdf

[6] Fann Instrument Company, "Model 35 Viscometer Instruction Manual", Houston, Texas, (2013).

[7] G.R. Gray, H.C.H. Darley, "Composition and Properties of Oil Well Drilling Fluids", Gulf Publishing Company, Houston, (1980), p 181-276.

[8] J.G. Savins, W.F. Roper, "A Direct-indicating Viscometer for Drilling Fluids", API Drill. Prod. Prac. (1954) p 7-22.

[9] G. Nygaard," PET525 Drilling Automation - Exercise 1: Simulating the Fann Model 35, a Couette type viscometer" (2014).

[10] K.L. Krogsæter," Automatic Evaluation of Drilling Fluid Properties Conventional and MPD Operations", University of Stavanger, (2013).

[11] Schlumberger, M-I SWACO, "Product Sheet: DUO-TEC NS", (2007). http://www.slb.com/resources/other_resources/product_sheets/miswaco/duo_tec_ns.aspx

[12] V.C. Kelessidis, R. Maglione, G. Bandelis, "On the en-effect correction for Couette type oil-field direct-indicating viscometers for Newtonian and non-Newtonian fluids", Journal of Petroleum Science and Engineering 71 (2010) 37-46.

[13] G. Nygaard, "PET525 Drilling Automation - Exercise 1 Solution" (2014).